This is to certify that the
thesis entitled

NEUROQUEST: A COMPREHENSIVE TOOL FOR LARGE-SCALE NEURAL DATA ANALYSIS

presented by

KI YONG KWON

has been accepted towards fulfillment
of the requirements for the

M.S. degree in ELECTRICAL ENGINEERING

Major Professor's Signature

05/10/2010
Date

NEUROQUEST: A COMPREHENSIVE TOOL FOR LARGE-SCALE NEURAL DATA ANALYSIS

By

Ki Yong Kwon

A THESIS

Submitted to
Michigan State University
In partial fulfillment of the requirements
for the degree of

MASTER OF SCIENCE

Electrical Engineering

2010

ABSTRACT

NEUROQUEST: A COMPREHENSIVE TOOL FOR LARGE SCALE NEURAL DATA ANALYSIS

By

Ki Yong Kwon

Processing the massive amounts of neural data to extract biologically relevant information from the activity of large ensembles of neurons in noisy recordings is a major challenge. Efficient and practical software development is indispensable to deal with these challenges, and many scientific findings will rest on the ability to overcome these challenges.

We developed a comprehensive MATLAB-based software package - entitled NeuroQuest - that bundles a number of advanced neural signal processing algorithms together in a user-friendly environment.

In this thesis, we also proposed novel spike detection and feature extraction algorithms that are fully integrated in NeuroQuest. These methods capture a number of useful features in a sparse representation domain of the neural signals. These sparse "footprints" permit efficient and reliable identification of neural spike events, even in the presence of interfering signals. Results demonstrate the efficiency and reliability of these methods compared to other similar methods and software packages, and versatility to a wide range of experimental conditions.

TABLE OF CONTENTS

LIST OF TABLES

LIST OF FIGURES

CHAPTER 1

Introduction

Recording and analyzing neurophysiological signals provide a window to understand how the brain interprets the physical world. This thesis presents NeuroQuest, a new software package for analyzing neurophysiological data, as well as novel spike detection and feature extraction methods implemented in the software. NeuroQuest is designed to assist researchers to translate recorded neural activity into quantitative measurements by combining a number of advanced neural signal processing algorithms in a unified Graphical User Interface (GUI). NeuroQuest is equipped to play an import role in processing the massive amounts of neural data to extract biologically relevant information about brain function. The algorithms are designed to improve the quality of the analysis. This chapter provides introduction of the study of neurophysiological signals, motivation for this work, the contributions, and an overview of the following chapters.

1.1 Study of Neurophysiological signals

Electrophysiology is the study of the electrical properties of biological cells and tissues. It involves measurements of voltage or current on a wide variety of

scales from single ion channel proteins to whole organs. In neuroscience, the study includes measurements of the electrical activity of neurons [1]. Recording action potentials - or spikes - emitted by neurons to signal each other is key to understanding the complex relationship between physical features of the world and the brain's interpretation of those features [2]. Neural data in the form of spikes from a single neuron or from populations of neurons have been extensively used in various studies, for e.g., to measure connectivity between different brain areas, to examine the dynamics of neuronal response and its relationship to external stimuli, to design Brain-machine Interface (BMI) systems, to clinically diagnose and treat brain disorders such as Parkinson's disease (PD) and certain types of epilepsy, and many other research areas. Despite the significance of extracellular recordings, there are many technical challenges in recording and processing the data [3-6]. For example, extracellular recordings require a surgery to implant the recording electrodes which causes a risk of complications and permanent tissue damages. Neurons can be easily injured, and perturbation of their immediate environment can affect their firing patterns [2]. In addition, recordings are typically contaminated by artifacts and other noise components. Therefore, the data must go through multiple steps of processing before any statistical analysis or information extraction can be done [7]. Despite the risk of the surgical procedure and the commonly observed instability in the recordings, studies of extracellular recordings seem indispensable to many basic and translational neuroscience researches [2].

1.2 Existing software packages and their limitations

Many techniques and algorithms have been developed to analyze extracellular recordings, and they can be categorized into two groups: spike sorting software and spike train analysis software as shown in TABLE 1-1.

Spike sorting software is designed to extract spike trains from the extracellular recordings, and it consists of signal processing tools, such as filtering, spike detection, and spike sorting. Spike sorting is the most computationally intense process in neurophysiological signal processing, and despite significant improvements, spike sorting remains an imperfect process [7]. These packages only extract spike trains and provide very basic spike train analysis tools. MClust and KlustaKwik are example tools that require detected spikes as input data [8],[9].

The second category of software is designed to evaluate the statistical characteristics of spike train data. The input data to these software packages is spike train data that a user must obtain from extracellular recordings using other spike sorting software.

TABLE 1-1. EXISTING SOFTWARE PACKAGES

Category	***Spike Sorting***	***Spike Train Analysis***
Software	MClust, KlustaKwik, Chronux, NeuroMAX, OSort, Wave_clus, etc	MatOFF, Spike Train Analysis Toolkit, FIND, etc

Very few academic software tools exist to date that integrate all the needed processing steps in one comprehensive package. As a result, every lab relies on custom built analysis tools in one form or another. This is coupled with a significant lack of community–wide standardized set of tools that enables replicating experimental data analysis across labs to facilitate objective comparison between scientific findings.

Automated processing is necessary to process large scale datasets, but it is inevitable to select some parameters manually in some situations such as low Signal-to-Noise ratios (SNR). Manual selection of large number of parameter is performed empirically, and this makes manual processing tedious and inconsistent.

1.3 Thesis Contributions

NeuroQuest is a MATLAB graphic user interface (GUI) software package developed in this thesis that contains a number of signal processing and analysis tools exclusively designed for extracellular neural recordings. NeuroQuest is distinguished from other software packages in several aspects:

First, the package includes algorithms for spike detection and sorting, as well as spike train analysis. This creates a unified processing environment that makes a sequence of processes and analyses more efficient and time saving.

Second, spike detection and sorting algorithms implemented in NeuroQuest outperform those in other software packages such as KlustaKwik, WAVE_CLUS, and OSort [8],[10],[11]. Robust spike detection and sorting are crucial because virtually all-subsequent neural data analysis depends on the outcome of these two steps. These two steps may vary in the way they are implemented depending on the type of electrode array used and brain area of recordings, and NeuroQuest offers multiple spike detection and sorting methods designed for different situations.

Third, the Graphical User Interface (GUI) of NeuroQuest reduces the complexity of selecting the large number of parameters needed during the analysis. This significantly reduces learning time for users. NeuroQuest also provides a variety of graphical tools to help the user manually set the parameters of choice by instantaneously illustrating the effect of parameter changes on the analysis results.

Fourth, individual modules are designed as independent GUIs. This design scheme allows a developer to integrate easily their own processing modules into NeuroQuest.

Finally, NeuroQuest provides advanced spike train analysis tools that enable identifying the functional and effective connectivity between simultaneously recorded cells. This is fundamentally important when studying cortical plasticity at the population level that may accompany learning and

memory formation - an important design consideration for neural decoding algorithms in adaptive BMIs.

1.4 Organization

The remainder of this thesis is organized as follows. In Chapter 2 the structure and the organization of NeuroQuest are presented. It further discusses the contribution of NeuroQuest to overcome the limitations of other software packages and summary of each process module of NeuroQuest. Finally in chapter 3, spike detection and spike sorting methods implemented in NeuroQuest are presented. This unique spike detection method utilizes sparse representation of the signal for better neural yields and more robust detection in low SNR cases.

CHAPTER 2

Background

This chapter presents a brief summary of neurophysiological signal processing. In section 2.1 different types of neurophysiological signal and their characteristics, applications, and limitations are presented. Section 2.2 presents the complete procedure of spike train analysis from extracellular recordings, as well as previous work on spike detection and spike sorting methods.

2.1 Neurophysiological signals and the characteristics

Electrophysiology is the study of the electrical properties of biological cells and tissues that involves measurements of electric potential and current changes. In neuroscience, the study focuses on measurements of the electrical activity of neurons, known as neurophysiological signals [1]. The commonly known types of neurophysiological signal are Electroencephalogram (EEG), Electrocorticogram (ECoG), and extracellular recordings, depending on the source of the signal and the recording sites [2]. EEG, recorded from the scalp, is the summation of the synchronous activity of large populations of cortical neurons. EEG has been extensively used in various fields such as neuroscience, cognitive science,

clinical applications, and Brain Machine Interface (BMI) mainly because of the advantage of being non-invasively recorded. However EEG suffers from poor spatial and temporal resolutions caused by the filtering effect of the skull and the artifacts from muscle movements [2].

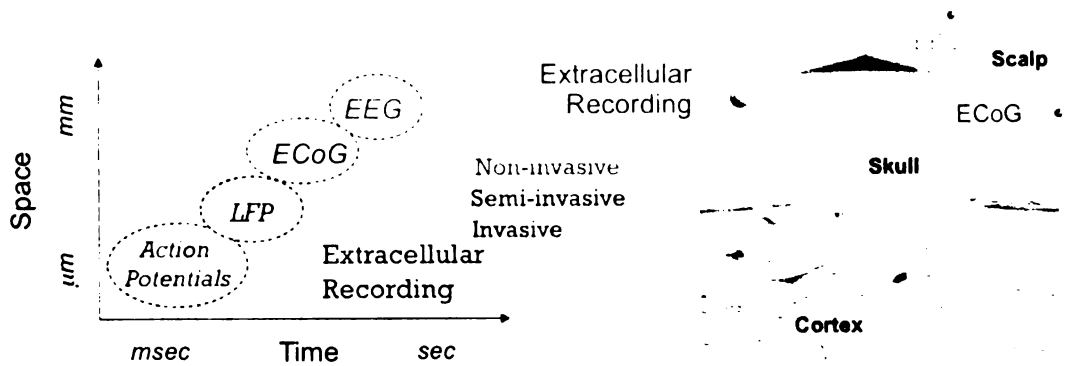

Figure 2-1. Types of neurophysiological signals adapted from [12]

The second type of signal is ECoGs and is directly recorded from the cortical surface to circumvent the rapid signal attenuation effect of the skull [2]. ECoG has higher spatial resolution, broader bandwidth, and higher amplitude than EEG, because the electrodes record the neural activity from a smaller brain area [13]. They are also free of muscle, eye-movement, and other artifacts consistently present in the scalp EEG of waking, moving patients. ECoG has been used to localize epileptogenic foci during pre-surgical planning, to map out cortical functions, and to predict the success of epileptic surgical re-sectioning [14],[15]. Although ECoG delivers these superior features, they are semi

invasively recorded, requiring a craniotomy, and therefore cannot be collected in healthy humans [2].

Extracellular recording - the observation of action potentials generated by a single or ensembles of neuron – can be obtained by directly implanting voltage-sensing microelectrodes. Extracellular recording typically contains two types of signals: Local Field Potential (LFP), and Action Potential (AP). LFP is believed to be the sum of action potentials generated by cells within approximately 50-350μm from the tip of the electrode [16]. LFP is obtained by low-pass filtering the recordingswith cutoff frequency at ~300Hz.

Action potentials - or spikes – constitutes the main communication method among neurons, and are key to understanding the complex relationship between physical features of the world and the brain's representation and interpretation of those features [2]. APs from a single or population of neuron have been used in various studies such as measuring connectivity between different areas of the brain, examining dynamics of neuronal response and their relationship to behavior, summarizing experimental data, BMI applications, clinical diagnosis of the brain disorders such as Parkinson's disease (PD) and certain types of epilepsy, the application of Deep Brain Stimulation (DBS), and many other research areas [3-6]. Despite the significance of studying extracellular recordings, there are technical challenges in recording and processing the data. Extracellular recordings require a surgery that causes a risk of complications and permanent tissue damage to implant the recording electrodes [2]. Since the

recordings are contaminated by artifacts and other noise components, the data must go through multiple steps of signal processing before the statistical analysis [7]. Despite the risk of surgical procedure and invasive and unstable recordings, studies of extracellular recordings seem indispensable to biomedical applications and basic research.

2.2 Extracting information from neural activity

Extracellular recordings must go through multiple steps of signal processing, *Pre-Conditioning, Spike Detection* and *Spike Sorting,* before examining the statistical property of the neural responses obtained.

2.2.1 Pre-Conditioning

Pre-Conditioning is a combination of processes to enhance the quality of the signal to make it suitable for further information extraction. The raw extracellular recordings are contaminated by many noise components such as 1) background neural activity attributed to neural sources far from the electrode array, 2) thermal and electrical noise produced by electrical devices in the data acquisition system, 3) other artifacts from muscle movement and mechanical noise [17]. The raw extracellular recording is filtered to remove low frequency

components such as LFP to be able to detect spikes. Artifacts that have similar spectral properties with APs as shown in figure 2-2 must be removed, because these artifacts could be incorrectly classified as spikes causing a decrease in accuracy of further analysis results. If the recordings suffer from low signal to noise ratio (SNR), various noise reduction techniques can be used to improve the SNR.

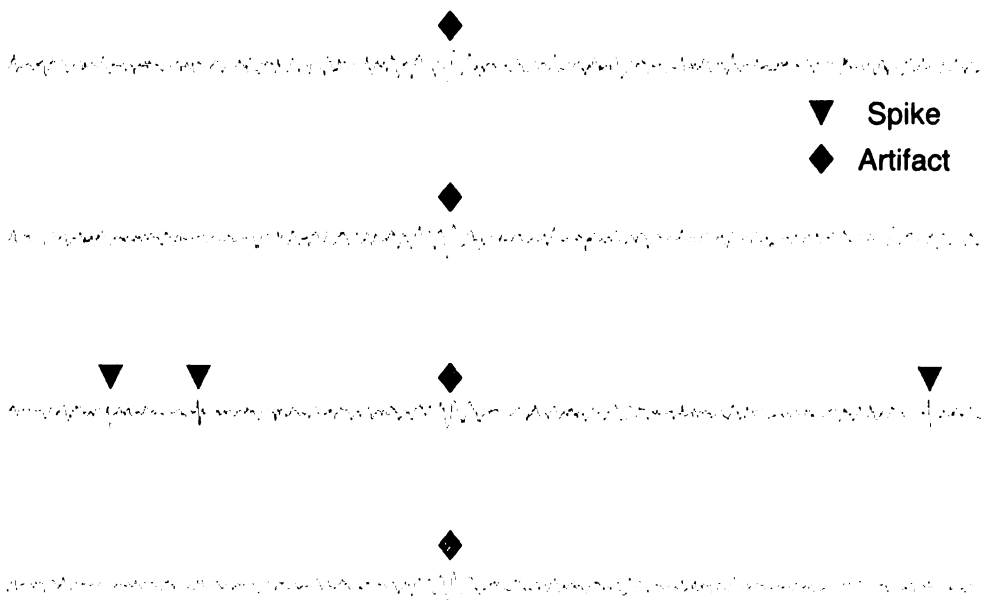

Figure 2-2. Artifacts and action potentials in the extracellular recording

2.2.2 Spike Detection

Detecting the presence of action potentials from the extracellular recording is referred to as *Spike Detection*. It is believed that spike arrival times carry all the information about information processing and not the actual waveform shape.

Therefore extracting the temporal information of spikes is a fundamental step in the analysis of neural recordings [2]. The main challenges in spike detection are the noisy environment of neural recordings and the similarity between the spike waveforms and the background noise. Many spike detection algorithms are available to overcome these challenges. The simplest technique for spike detection is amplitude thresholding that searches for an event that crosses user-specified amplitude thresholds [7]. Although its computational simplicity that makes easy to implement in hardware, the performance of the method declines rapidly in low SNR. The instantaneous energy of an extracellular signal has been used to emphasize the spike peak [18],[19]. This method is more robust to the noise than the amplitude threshold method, but the energy computation without any noise reduction technique causes a poor performance in low SNR. In template matching method, templates, obtained during a training session, are used to locate possible events in the signal by measuring the resemblance between the template and the segments of the signal [18]. This method relies on *a priori* knowledge of the spike shape to form the template. The performance again decreases in low SNR, since the automatic selection of a template in a noisy signal is very difficult. Transformation and decomposition of signals are also used in spike detection methods. Spike features, observed in the wavelet domain, have an advantage that separates signals from noise by thresholding the wavelet coefficients [10],[20],[21]. The wavelet based spike detection methods suggest that sparsity plays an important role in spike detection by

increasing the SNR. The main drawback of this technique is the assumption of a similarity between a family of wavelet base and a spike shape.

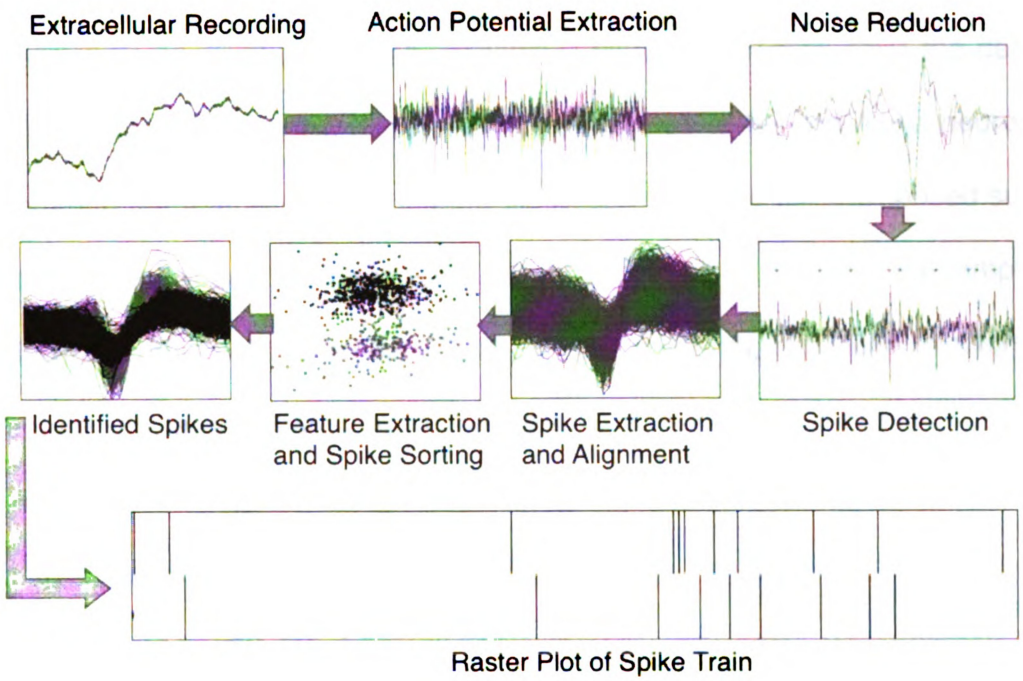

Figure 2-3. Processes to obtain spike train from extracellular recording

2.2.3 Spike Sorting

As the tip of the electrode is surrounded by many neurons, the extracellular recordings can simultaneously pick up spikes of an unknown number of neurons. The detected spikes can be assigned into a particular neuron. This process is called *Spike Sorting,* and this is valid under the assumption that each neuron generates a distinguished spike shape from others

[7]. Spike sorting methods are categorized into two approaches: 1) The pattern recognition approach: operates on the individual spikes extracted after the spike detection step; 2) The Blind Source Separation (BSS) approach: operates on the raw data without the need to perform spike detection a priori [12]. The Pattern recognition approaches typically consist of feature extraction from the detected spike waveforms and the assignment of the spikes to the individual neurons by clustering the features. Many feature extraction methods were proposed such as feature of the shape, such as spike height and width or peak-to-peak amplitude, principal component analysis (PCA), a set of orthogonal basis vectors that capture the largest variation in the data, and Wavelet Transform [7],[10],[22]. These extracted features are clustered using unsupervised classification methods such as hierarchical clustering, k-means and fuzzy c-means, Gaussian mixture model and the t-distribution mixture model, and self organizing map [7],[23-26]. K-means clustering is relatively sensitive to outliers, and mixture model based clustering methods usually need assumption of certain distribution to yield accurate clustering results. The clustering is data-driven process which means that there is no absolutely superior clustering method than others. Each of clustering method is designed for the certain type of data, and a proper clustering method must be selected regarding the nature of the data to yield an optimal clustering result [27].

In BSS approach, the observation signal is considered to be a mixture of multiple signals, and the original signals can be estimated from the mixture by

finding the unmixing weights [7]. Independent Component Analysis (ICA) and Multiresolution Analysis of Signal Subspace Invariance Technique (MASSIT) are examples of the BBS approach [28],[29]. Spike sorting has become crucial in multiple spike train analysis, because the accuracy of spike sorting influences the validity of subsequent analysis [6].

2.2.4 Spike Train Analysis

Statistical properties of population of neuron are estimated using the temporal arrival time information of identified neurons [6]. Action potentials can be represented a stream of binary events, or called a spike train, where '1' represents the arrival of spike and '0' is not. Spike trains are widely used in the study of neurophysiology especially neural coding, characterizing the relationship between the stimulus and the individual or ensemble neuronal responses and the relationship among electrical activity of the neurons in the ensemble [2],[5],[6].

Spike train analysis is the attempt to find patterns in spike trains that reflect some aspect of neural functioning. This could include relating neural activity to stimuli, finding functional interactions among neurons, and estimating codes distributed across a neuron population [30].

2.2.4.1 Single Neuron Properties

One of the simplest ways to study the patterning of spike activity of a neuron is to construct an interspike interval histogram (ISIH). This is simply a plot of the distribution of the observed times between spikes collected in fixed width [5]. Peristimulus Time Histograms (PSTH) are histograms of the times at which neurons fire. These histograms are used to visualize the rate and timing of neuronal spike discharges in relation to an external stimulus or event [31].

2.2.4.2 Multi Neuron Properties

The cross-correlogram is a function that indicates the firing rate of one neuron versus another. Cross-correlograms give a measure of the firing rate of one neuron around the time that another neuron fires which indicate the dependency of the pair neurons [32].

Joint Peristimulus Time Histogram (JPSTH) gives not only the ability of cross-correlograms, but also displays the stimulus-related dynamics of the relationship. The temporal information that is given by the two-dimensional nature of the JPSTH is important in studying neural connectivity [33].

Advanced analysis tools consist of identifying relationships between the observed neurons from spike train ensembles. NeuroQuest offers two algorithms to achieve that goal: *multiscale clustering* and *Dynamic Bayesian Network* (DBN). The first algorithm identifies any potential statistical dependency between spike trains, often referred to as functional connectivity [34]. The second algorithm

infers the type of connection (excitatory/inhibitory) and directions between the functionally-interdependent neurons, often referred to as effective connectivity [35]. This is achieved through DBN. This two-stage framework can efficiently identify neural circuits in large neuronal populations. It can also be utilized to track plastic changes associated with learning and memory.

CHAPTER 3

Overview of NeuroQuest

This chapter provides context for the contributions of the thesis. First, the structure of NeuroQuest and the organization of individual processing modules are presented in Section 3.1. Second, Section 3.2 discusses the contributions of NeuroQuest that overcome the limitations of current existing software packages. Finally, summary of individual process modules are presented in Section 3.3.

3.1 Structure and Organization of NeuroQuest

NeuroQuest is designed to process the large-scale raw extracellular recordings to obtain dynamics of neural population with statistical tools. NeuroQuest bundles multiple processing modules designed as Graphical User Interface (GUI), and they are connected to each other through the main workspace as shown in figure 3-1. Total 8 processing modules provided in the software are classified into two groups: spike sorting group and spike train analysis group. Spike sorting modules require the raw or pre-processed extracellular recordings, while spike analysis tools handle single or multiple spike trains. Once the input data is loaded, the corresponding group of modules becomes available on the main menu. Each module contains sub-modules that assist to yield more accurate analysis results.

Figure 3-1 illustrates the organization of the individual processing modules and their sub-modules of NeuroQuest. Details of each process are discussed in section 3.3.

The flowchart in Figure 3-2 demonstrates the complete neural data processing and analysis steps in NeuroQuest. After the extracellular recording data is loaded, the group of spike sorting tools is activated for further process. The first stage is to denoise the data to enhance the neural yield. After denoising, spikes are detected from the recording. Detected spikes are extracted from the data and sent to the spike sorting algorithm to obtain spike trains. The obtained spike trains are then further analyzed using the primary spike train analysis tools such as Interspike Interval Histogram(ISIH), Peristimulus Time Histogram(PSTH), Joint Peristimulus Time Histogram(JPSTH), Cross-Correlogram (CC), and the advanced spike train analysis tools such as functional and effective connectivity estimation among observed neural population. Since individual modules are designed as an independent GUI, the analysis results of each module can be saved and loaded separately for the later data analysis.

3.2 The contributions of NeuroQuest

The main contribution of NeuroQuest is to provide a tool that assists a researcher to translate neural dynamics into statistical measurements. Many

neurophysiological signal processing software packages were developed for the purpose , but they did not fulfill the needs with their limited capabilities to deal

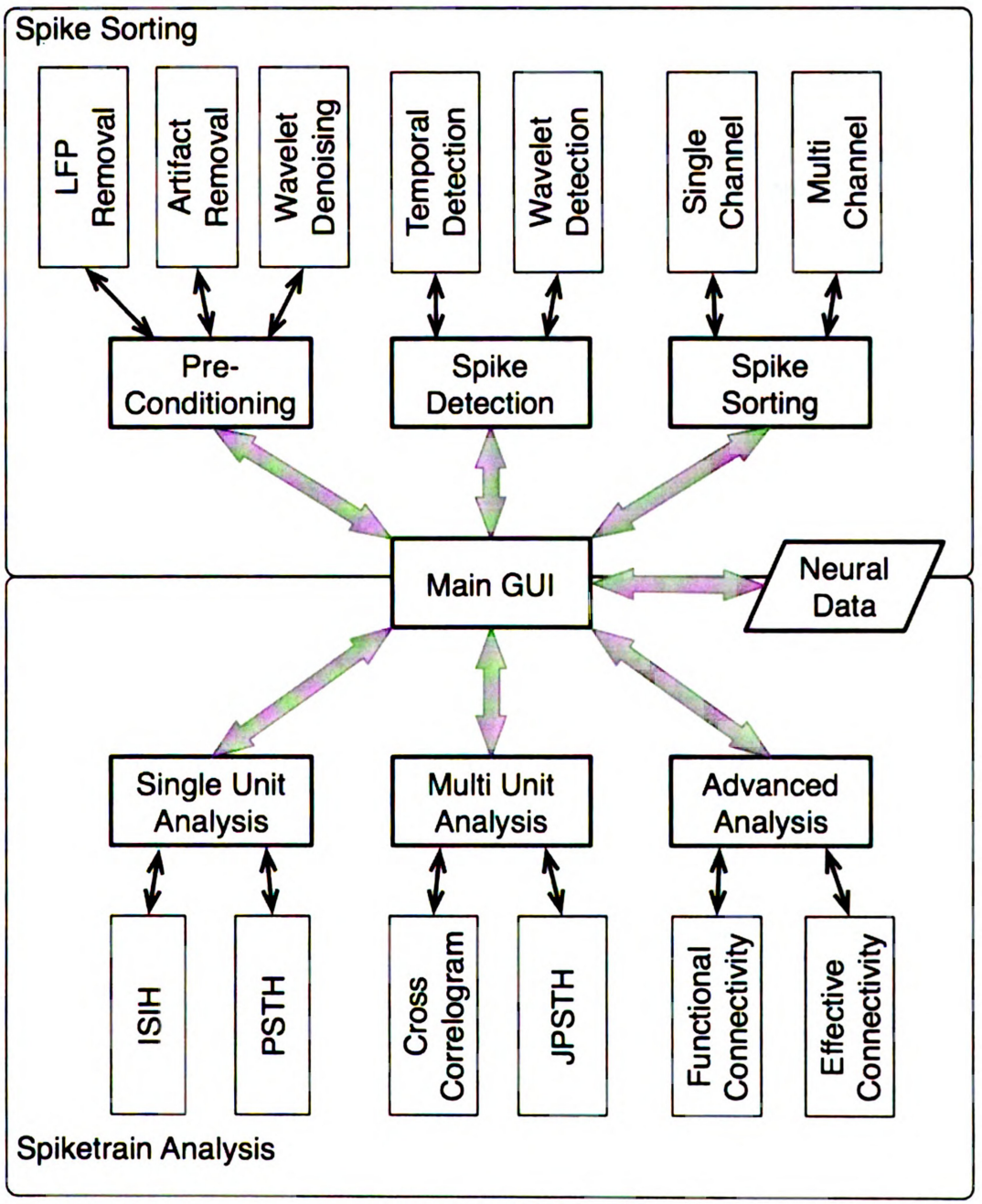

Figure 3-1 Organization of NeuroQuest

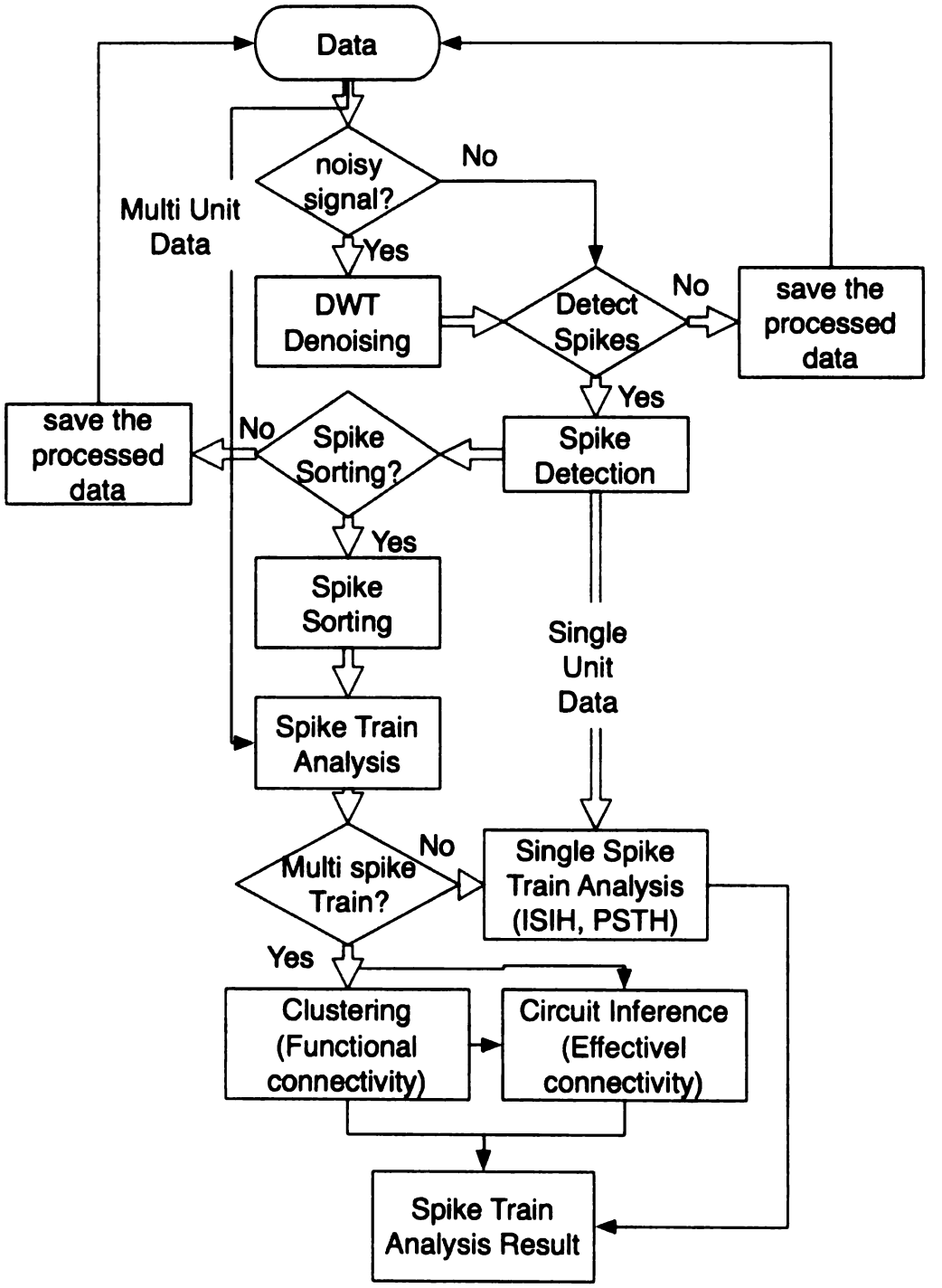

Figure 3-2 Flow Chart of NeuroQuest

with the experimental data. NeuroQuest is designed to overcome the limitations of the existing software packages, and following aspects make NeuroQuest distinguished from the others: 1) comprehensive toolbox, 2) simple GUI and visualization tools, 3) capability of handling large-scale neural data, 4) varieties of spike detection and sorting methods, and 5) developer friendly environment.

3.2.1 Comprehensive toolbox

As mentioned in chapter 1, most of the current existing software packages fall into two groups, spike sorting software and spike train analysis tools. Since both groups are required to perform a complete neural data analysis, a combination of multiple software packages is used to analyze experimental data. However this scheme has several drawbacks. First of all, input data must be converted into suitable format for the different software packages, since each software package requires different input data format. It is also time consuming and inefficient process due to the stream of non-unified processes for the single analysis. TABLE 3.1 illustrates the provided features of several software packages available. Among spike sorting software, only NeuroMAX and OSort offer limited spike train analysis tools [11]. Among spike train analysis tools FIND is the only software equipped spike detection and simple spike sorting tools [36].

NeuroQuest offers comprehensive tools from pre-processing of extracellular recordings to analyzing multiple spike train to achieve seamless

TABLE 3-1. FEATURES OF THE SOFTWARE PACKAGES

	Chronux	KlustaKwik	MClust	NeuroMAX	FIND	MatOFF	STAToolkit	Wave_Clus	OSort	NeuroQuest
GUI	✔	✔	✔	✔	✔	✔	✔	✔	✔	✔
Pre-Conditioning	X	X	X	X	X	X	X	X	✔	✔
Spike Detection	X	X	X	✔	✔	X	X	✔	✔	✔
Spike Sorting	✔	✔	✔	✔	X	X	X	✔	✔	✔
Single Unit Analysis	X	X	X	✔	✔	✔	✔	X	✔	✔
Multi Unit Analysis	X	X	X	X	✔	✔	✔	X	X	✔
Connectivity Estimation	X	X	X	X	X	X	X	X	X	✔

neural data analysis. This seamless and unified process eliminates the burden of converting data and speed up the analysis.

3.2.2 Simple GUI and Visualization Tools

A large number of parameters selections are required in each step of the analysis and the complexity of the parameter selection increases the learning time of the software for the users. The simple GUI of NeuroQuest reduces the complexity of the parameter setting and shortens the learning time. Various graphical tools help

the manual parameter selection by instantaneously illustrating the effect of the parameter changes on the analysis results. The extensive visualization of the manual process helps to improve the accuracy of the analysis results. We demonstrate the effectiveness of the GUI by comparing the spike detection result against OSort, a spike sorting software package, using the same energy-based spike detection method with three simulation data sets obtained from the OSort package [11].

Detection Rate is defined as a total number of positive detection over a total number of the actual spikes. As Figure 3-1 shows, NeuroQuest yields more reliable positive spike detection results with various noise levels while maintaining the same false detection rate. Details of the spike detection comparison between NeuroQuest and OSort results are found in TABLE 3-2. The improved detection performance is due to the threshold selection tool in the spike detection GUI that assists a user to select a proper threshold.

3.2.3 Capability of handling large-scale neural data

Complex behavioral related experiments require hours of data recordings, and processing these data become another challenge in neuroscience and BMI development [7]. Most of existing spike sorting tools are missing the capability of handling large-scale neural data mainly due to the MATLAB environment

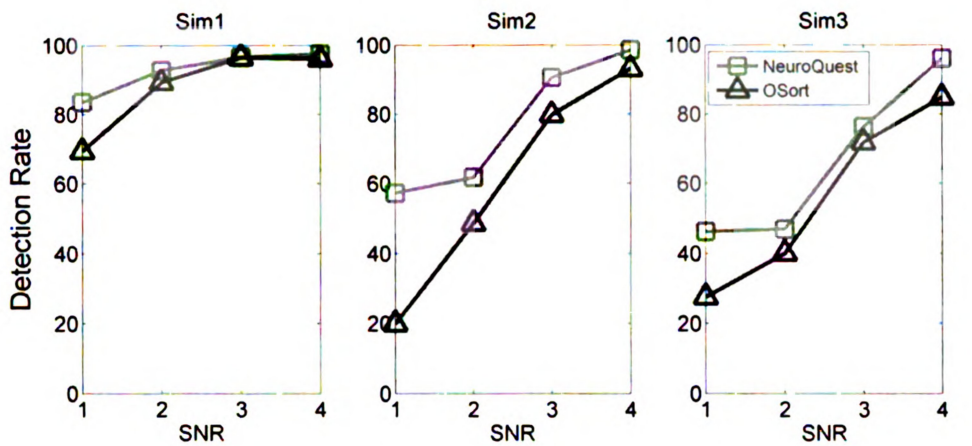

Figure 3-3. Comparison of Spike Detection performance between NeuroQuest and OSort

TABLE 3-2 SPIKE DETECTION RESULTS OF NEUROQUEST AND OSORT WITH FOUR SIMULATION DATASETS

SNR	4	3	2	1
Sim1 (1576)	TP:1535 (97.40%) FP: 0	TP:1523 (96.57 %) FP: 0	TP:1463 (92.83%) FP: 13	TP:1316 (83.50%) FP: 75
	TP:1513 (96%) FP: 0	TP:1503 (95.37%) FP: 2	TP:1407 (89.28%) FP: 46	1094 (69.42%) FP: 163
Sim2 (1568)	TP:1544 (98.47%) FP: 0	TP:1420 (90.56%) FP: 39	TP:967 (61.67%) FP: 85	TP:857 (57.27%) FP: 225
	TP:1460 (93.11%) FP: 0	TP:1251 (79.78%) FP: 14	TP:762 (48.60%) FP: 202	TP:312 (19.90%) FP: 134
Sim3 (2986)	TP:2870 (96.12%) FP: 6	TP:2278 (76.29%) FP: 60	TP:1400 (46.89%) FP: 321	TP:1378 (46.15%) FP: 348
	TP:2531 (84.76%) FP: 7	TP:2145 (71.84%) FP: 317	TP:1193 (39.95%) FP: 270	TP:820 (27.46%) FP: 308

The shaded area indicates the results of NeuroQuest and the white background is the result of OSort.

,known for poor handling of large dataset, and this is a significant drawback in the process of the experimental data. Although NeuroQuest also runs on MATLAB environment, we circumvent the memory issue by allocating large data set into small segments. This segmentation helps to speed up the process and resolves the 'out of memory' problem. The segmented process also helps to improve the accuracy of the analysis results by estimating the important parameters for the process locally.

3.2.4 Spike Detection and Sorting methods

Some characteristics of extracellular recordings, caused by the different geometry of the recording electrode array, require specially designed processing technique. Most of the software packages only offer single spike sorting method that is not suitable for processing the different types of data. NeuroQuest is the only software that offers array detection and sorting algorithms that are specially designed to analyze the data recorded using the closely spaced electrode array such as stereotrodes, tetrodes and polytrodes.

3.2.5 Developer Friendly Environment

Very few software tools exist to date that integrate all the needed processing steps in one comprehensive package. As a result, every lab relies on custom

built analysis tools in one form or another. This is coupled with a significant lack of community–wide standardized set of tools that enables replicating experimental data analysis across labs to facilitate objective comparison between scientific findings. In NeuroQuest individual modules are designed as an independent GUI, and this design scheme allows a developer to integrate their own processing module into NeuroQuest easily for the performance comparison.

3.3 Summary of individual modules

3.3.1 Data format

Since most of the commercial extra-cellular recording systems store the recordings with their own data structure, proper data conversion is the inevitable step to use the academic software packages. Without a standard data format, data conversion is one of the difficulties in the development of neurophysiological signal processing tools. There have been a consensus on unifying data structure of neurophysiological recordings, and NeuroShare (http://**neuroshare**.org/) is one of the many efforts. This data structure is designed to efficiently store neurophysiological signals, and several commercial and academic software packages are supporting this format. However the NeuroShare data converter requires mediate levels of understanding in computer language C++.

To make usage of the software more universal, a generic MATLAB data file is used for the input data of NeuroQuest. NeuroQuest works with a MAT file that contains a specific data structure (see Appendix A) that can be created easily with a beginner level of understandings in MATLAB script language. Once the following components are saved in a MAT file, NeuroQuest automatically enables the group of modules that can be applied to the data.

3.3.2 Pre-Conditioning

Pre-Conditioning tools are designed to improve the quality of data and preserve the information at the different frequency range other than APs (frequency range of 300Hz - 5000Hz) such as LFP. Properly pre-conditioned data improve the SNR and fewer artifacts that increase the accuracy of further processes such as spike detection and spike sorting. Three pre-conditioning tools in NeuroQuest, LFP Removal, Artifact Removal, and Wavelet Denoising are presented in this section.

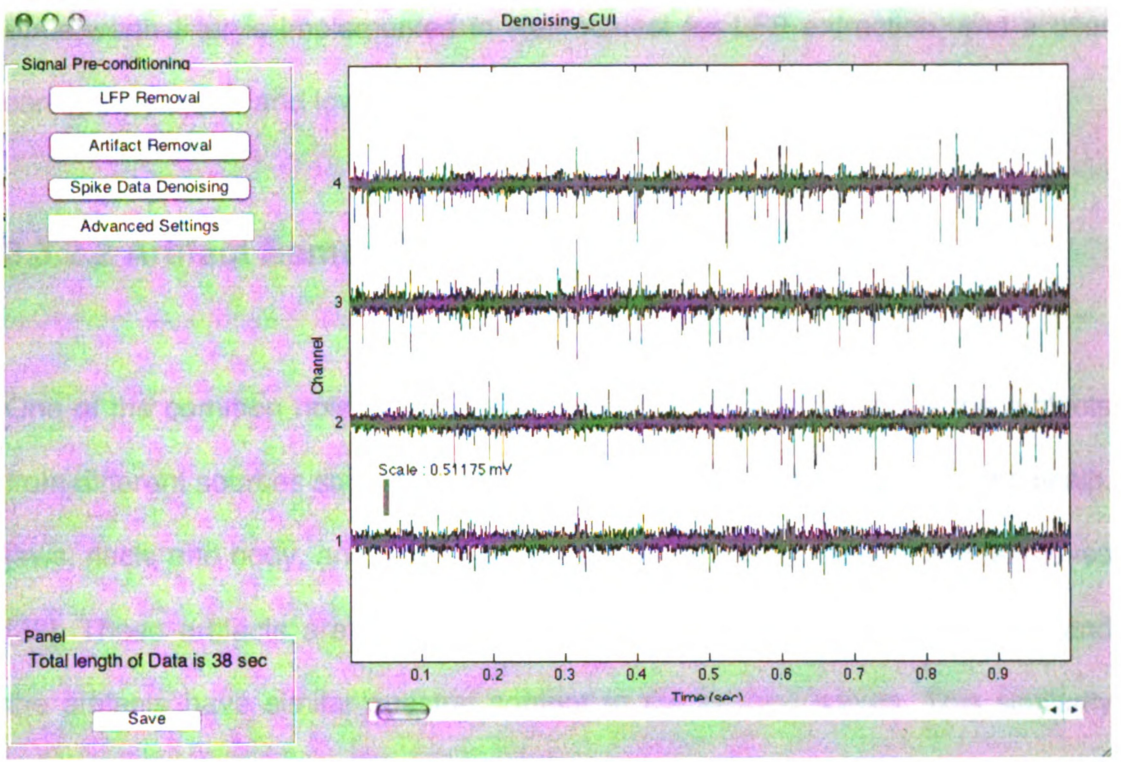

Figure 3-4 Pre-Conditioning GUI

3.3.2.1 LFP Removal

LFP is low frequency oscillation, range of 0Hz - 300Hz, that measures the activity in a population of neurons. LFP is robust over time comparing with AP, while it provides highly specific information [2]. Conventionally LFP was considered as a noise component and filtered out from the recordings [7]. However current studies show that LFP has excellent decoding properties for Brain Machine Interface and other studies [2]. NeuroQuest extracts LFP data from the unfiltered extra-cellular recording and displays it using a spectrogram [37]. 5^{th} order

Butterworth filter is implemented in NeuroQuest for LFP extraction, and a user can specify upper and lower band limits of the filter [38].

3.3.2.2 Artifact Removal

One of the common noise components in extra-cellular recording is the artifacts from different sources such as electromyogram (EMG) from muscles in the scalp, jaws, neck, and body, and many types of electrical artifacts as the animal moves [39]. These artifacts are highly correlated through neighboring electrodes, and the artifacts have similar spectral content to the desired spikes. This similarity causes cluster overlap in feature space that make difficult to define clean boundaries for spike sorting. These artifacts can be identified using principle components analysis (PCA). First two or three PCs, the best representation of the data, reflect the correlated noise components and the artifacts can be removed from the recordings by eliminating these dominant PCs. Details of the method are found in [39].

3.3.2.3 Wavelet Denoising

Multi-electrode arrays are intended to simultaneously monitor large number of neurons and therefore detection of as many neurons as possible from the recorded signals is of fundamental importance. Effective denoising improves the

results of further signal processing steps, such as spike detection and spike sorting [9].

Spatially-correlated noise across channels is one of the fundamental problems faced during spike detection. It arises due to the synchronized firing of large cell assemblies that are not close enough to the recording array to be individually detected. Suppressing this noise component is necessary for optimal spike waveform detection. Conventional linear filtering methods, such as Fourier transform-based filters, are not suitable to discriminate this noise component from the signal of interest [9]. The Discrete Wavelet Transform (DWT) is a nonlinear transform that possesses many desirable properties not present in linear filtering methods. The DWT is a powerful signal processing tool that has been demonstrated to have excellent properties in many applications of denoising and compression with relatively simple mathematical computations [40],[41],[17],[20],[10].

For example, in the DWT domain, the signal is concentrated in very few coefficients with large amplitude while small amplitude noise coefficients are widely spread. This characteristic of DWT permits to suppress the noise by thresholding small coefficients. The performance of DWT denoising depends on the choice of the threshold. Six different thresholding methods are provided in NeuroQuest: Heursure, Rigrsure, VisuShrink, SureShrink, BayesShrink, and Minimaxi. Details of these methods are found in [40],[42],[43].

3.3.3 Spike Detection

The compactness property of the wavelet transform facilitates the detection of neural spikes in the wavelet domain. NeuroQuest performs multi-level stationary wavelet packet decomposition (SWT) of the recorded data. It uses a likelihood-ratio test (LRT) for detection, in which a sufficient statistic is computed depending on the array geometry [44],[45].

If the array is closely spaced, the statistic is computed from a snapshot of the entire array to minimize the effect of the spatially correlated noise component. If the array is not closely spaced, then the sufficient statistic is computed from snapshots of individual channels and therefore improves spike detection in both single and multi channel scenarios [41]. Not only wavelet detection, NeuroQuest also provides three time domain detection methods: single amplitude, absolute amplitude, and energy-based. Single amplitude detection method identifies any signal that crosses the threshold as a spike, while absolute amplitude detection applies both positive and negative thresholds simultaneously [7]. Energy-based spike detectors compare the local power of the signal with a threshold estimated from the power of noise [19]. This method is more robust to the noise than the amplitude threshold methods.

Several detection tools help to maximize detection performance. Manual detection allows a user to select a threshold value from the selected data segments. Different data segments, the lowest SNR, the smallest noise variance,

and a large data segment (30 sec of data segment is selected empirically) can be selected for the threshold value estimation. In wavelet detection, choices of different wavelet bases help to maximize the compactness of wavelet coefficients.

3.3.4 Spike Sorting

Spike sorting is a step where spikes are assigned to the individual neurons that have emitted them [7]. Overall spike sorting algorithm in NeuroQuest is described in figure 3-6.

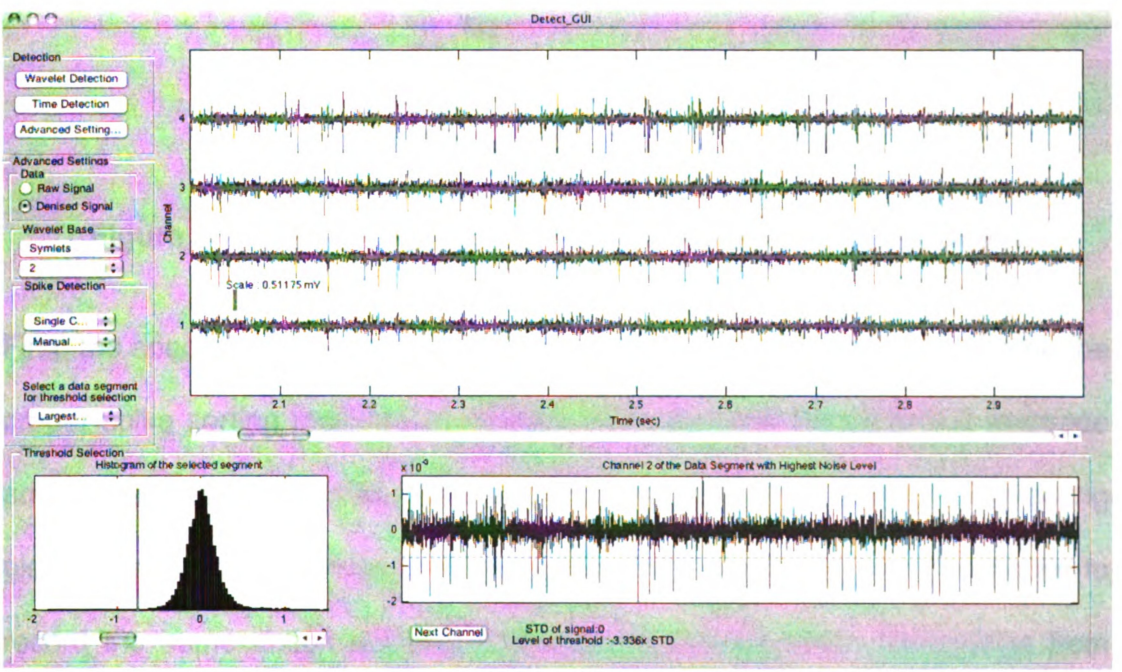

Figure 3-5. Spike Detection GUI

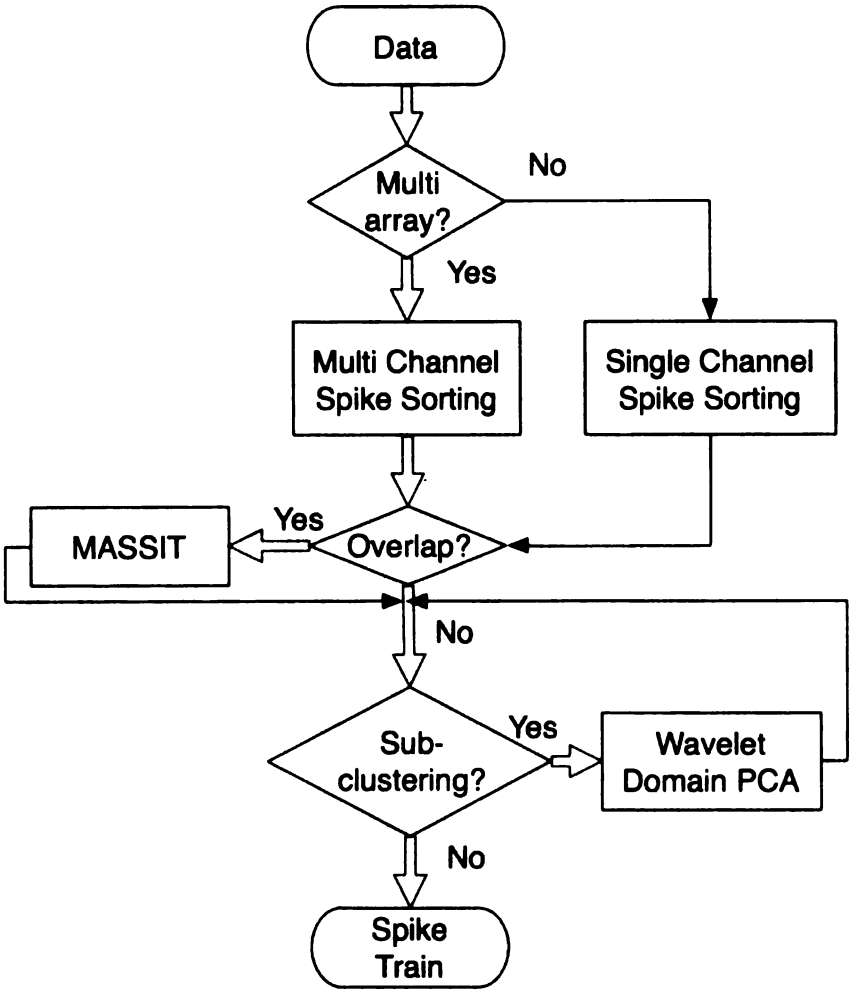

Figure 3-6. Flowchart of Spike Sorting Algorithm in NeuroQuest

First, the specific type of the recording electrode must be specified to choose the proper spike sorting method. Geometrical differences of the recording electrode array require different spike sorting approaches. If spacing between neighboring electrodes is close such as stereotrodes, and tetrodes, there is high chance to record the same action potential with a group of electrodes. Recordings from these electrodes allow additional information to be used for more accurate spike sorting [15]. Two types of spike sorting techniques, single and multi channel

sorting, are embedded in NeuroQuest. Single channel sorting method does not consider any correlation between the recordings from the adjacent electrodes and processes individual signal independently, while multi channel sorting captures the correlation among multiple electrodes and use the information to identify the source of the spikes.

Second, if two adjacent events are close enough, the event is considered to be an overlap. In the case, Multiresolution Analysis of Signal Subspace Invariance Technique (MASSIT) resolves the spike overlap based on an augmented representation of the observation space to simultaneously incorporate the spectral, temporal and spatial information of the spike waveform [44].

The algorithm verifies whether the detected events consist of a simple spike or overlap of two or more spikes. In the non-overlapping case, wavelet features of the spike waveform are compared to previously extracted features during training. If matching occurs, the spike is classified to belong to the matching class. If not, a new class is created. More details are provided in [44]. Spike sorting in NeuroQuest consists with three steps: spike extraction, feature extraction and clustering. Details of each step are discussed below.

3.3.4.1 Spike Extraction and Alignment

Detected spikes are extracted and aligned in this step. Since duration of spikes may vary, proper spike extraction is crucial to preserve the information for spike sorting. Spike alignment is also important factor in accurate classification [7].

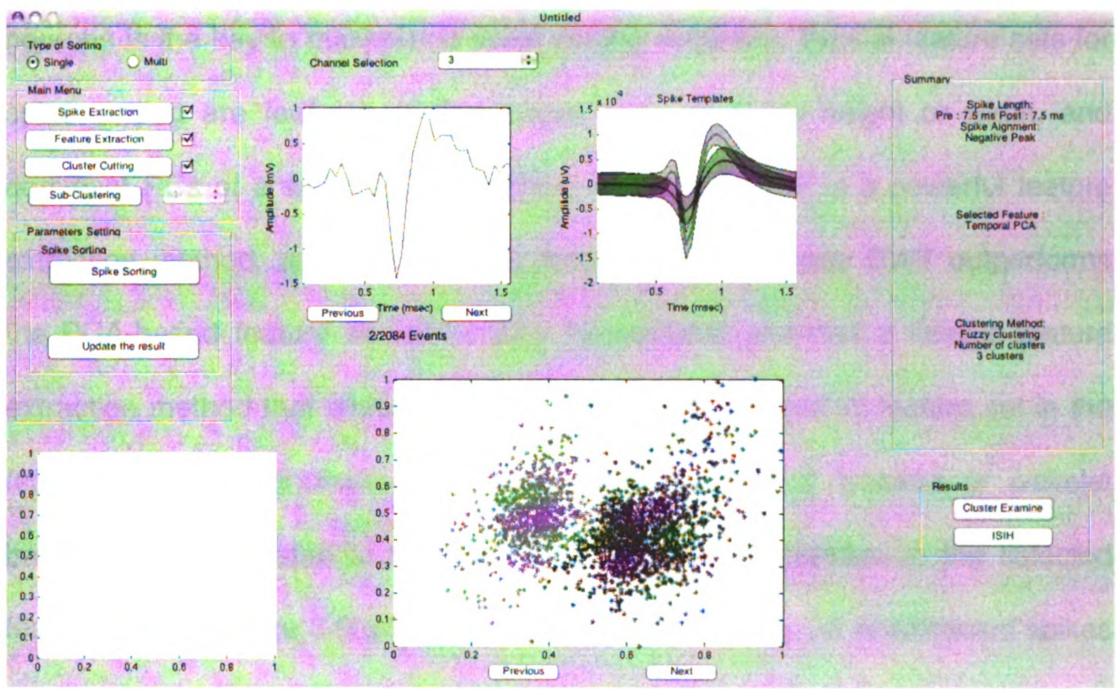

Figure 3-7. Spike Sorting GUI

(a) Negative Peak Alignment (b) Positive Peak Alignment (c) Energy-Based Alignment

Figure 3-8. Clusters of detected spikes in temporal PCA feature space with different alignment methods.

3.3.4.2 Feature Extraction

Next step is feature extraction from the properly extracted and aligned spikes. Extracting a feature set that represents a group of spikes emitted from the same neurons is the key to maximizing spike sorting accuracy. Typical feature sets for spike sorting are features of the shape, such as spike height or width, and dominant PCs of a spike. Recent studies show that DWT is a powerful feature extraction method, and with properly selected wavelet base DWT outperforms the PCA-based feature extraction [46]. NeuroQuest provides a flexible feature extraction method that allows a user to visualize the extracted feature set in the feature space instantaneously; different combinations of features or wavelet bases can be adjusted to achieve the best cluster separation in the selected feature space. Figure 3-9 shows the clusters of the same set of extracted spikes with the different feature sets. Wavelet footprint is a wavelet feature set that represents the transient of the spike by extract the largest wavelet coefficients through the nodes within a certain range or called the cone of influence [47]. Details of the method are discussed in chapter 4. As mentioned in chapter 2, properly selected wavelet base DWT, in this example Symlet wavelet base with scale 4, outperforms the PCA-based feature extraction by clearly forming 4 clusters while only three clusters appear in the temporal PCA domain.

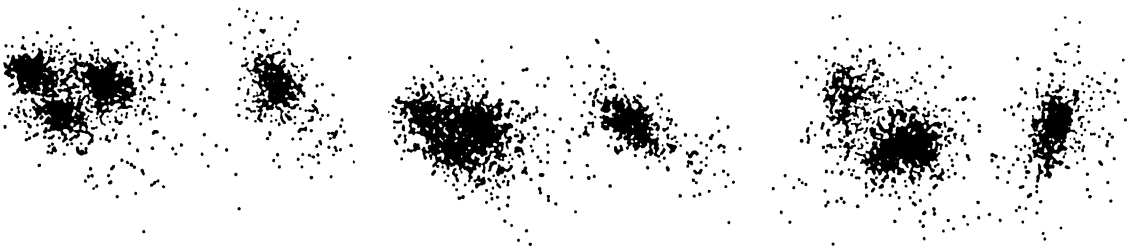

a) Wavelet footprint with sym4 wavelet base

a) Wavelet footprint with db4 wavelet base

a) Temporal PCA

Figure 3-9. Clusters of extracted spikes in different feature spaces.

3.3.4.3 Clustering

Clustering is a method for finding clusters in multidimensional data sets and classifying data based on those clusters. There are many methods for clustering and the best clustering method is driven by the nature of the data [27]. Estimating the number of cluster is one of the difficulties in clustering, and the automated class selection can yield a reasonable estimation only in certain condition such as sufficient cluster separation and accuracy of assumption of the distribution model [27]. Among many class estimation methods NeuroQuest employs the modified Expectation-Maximization (EM) algorithm for the class estimation method. This specific algorithm can be applied to any type of parametric mixture model for which it is possible to write an EM algorithm, while most of the literature on finite mixtures focuses on Gaussian mixtures [48]. Clustering of the extracted features is achieved through four clustering methods: Fuzzy c-means, EM, k-mean and manual cluster cutting [27],[25].

3.3.4.4 Sub-Clustering

Once the spike sorting is performed, initially classified classes can be further sorted into smaller classes using sub-clustering algorithm. Sub-clustering algorithm allows selecting one of the classified classes, and projects them into the different angle of the original feature space or a different feature space. If there is any improvement in cluster separation in the new feature space, new clusters are classified using the different clustering methods. Details of sub-clustering are illustrated in figure 3-10.

3.3.4.5 Extra spike sorting tools

NeuroQuest also provides two graphical tools to evaluate and enhance the spike sorting result. Interspike Interval Histogram (ISIH) is used to validate the sorting result, since a significant number of interspike interval within the refractory period indicates an error of the sorting results. Another assistant tool is class merging GUI that allows merging multiple classified classes into single class.

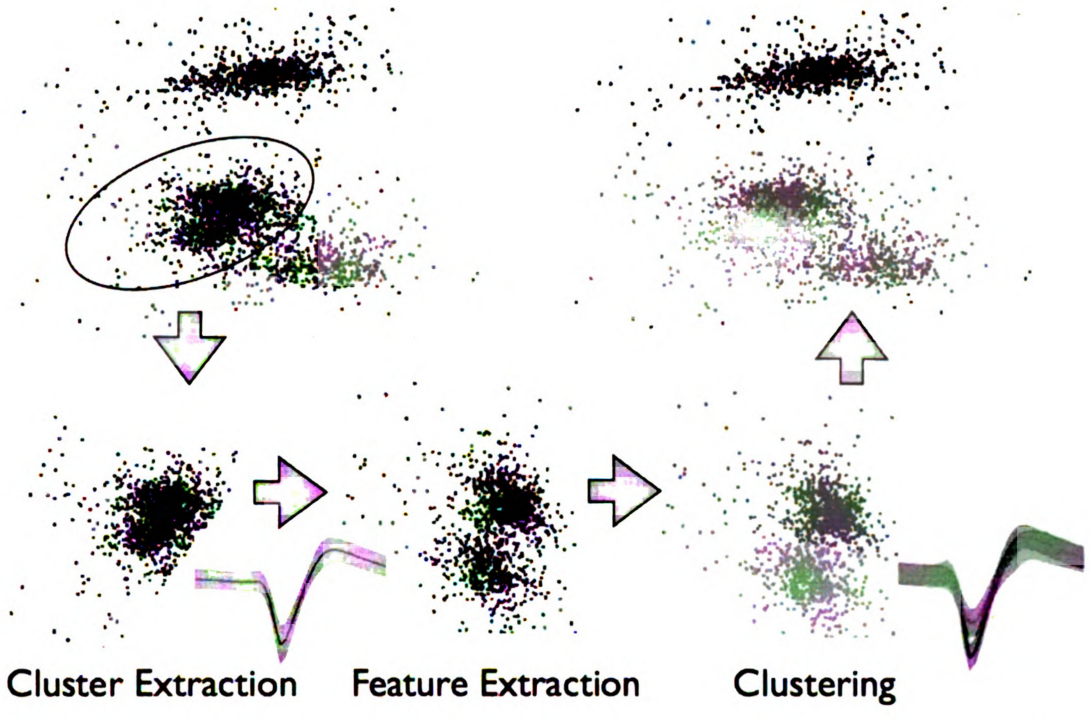

Figure 3-10. Scheme of Sub-Clustering.

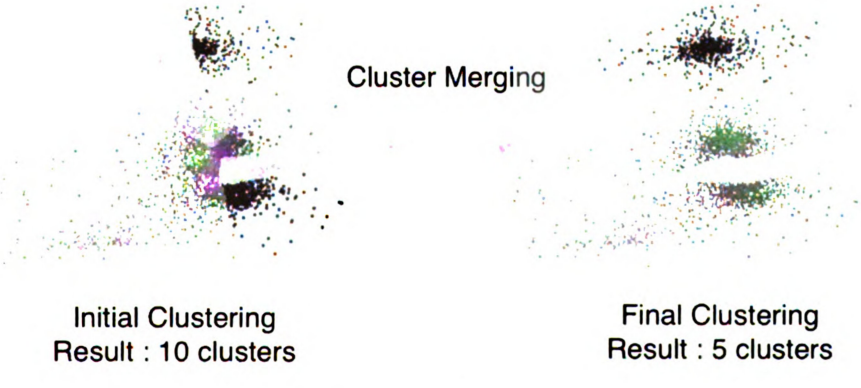

Figure3-11. Example of Cluster Merging Tool

Merging tool helps to correct the clustering error without re-clustering entire data. Merging tool can be also used as a manual clustering tool by initially clustering data into many classes and combining them. In figure 3-11 initially clustered 10 classes using Fuzzy-c mean are merged into 5 clusters.

3.3.5 Spike train analysis

Since it is believed that the time of arrival of the spikes carries all the information, the spike waveform is abstracted into a stream of binary events where an isolated '1' represents an action potential [6]. The binary waveform is referred to as a spike train. The patterns of spike activity are influenced by three things: a) the intrinsic properties of the neuron, especially the properties of its membrane, b) network interactions, because spike activity in one neuron might have feedback effects on that neuron because of the changes that it produces in reciprocally connected neurons and c) the nature of the inputs to that neuron [5]. Spike train analysis is the attempt to find patterns in spike trains. NeuroQuest provides a number of spike train analysis tools categorized into three groups: single unit analysis (SUA), multi unit analysis (MUA), and advanced analysis tools.

3.3.5.1 Single Unit Analysis tools.

One of the simplest ways to study the patterning of spike activity in a neuron is to construct an ISIH. This is a plot of the distribution of the observed times between spikes collected in 'bins' of fixed width.

PSTH, a histogram of the times at which neurons fire, is used to visualize the rate and timing of neuronal spike discharges in relation to an external stimulus or event. Let $n_i^{(k)}(u)$ be the spike count of neuron *i* in the *u*th bin of the *k*th trial. Then, the average spike count,

$$\langle n_i^{(k)}(u) \rangle = \frac{1}{K} \sum_{k=1}^{K} n_i^{(k)}(u) \tag{3.1}$$

represents the probability of the occurrence of the spike event of neuron *i* at bin u, where K being a total number of trials. The histogram of $\langle n_i^{(k)}(u) \rangle$ over index u represents the PSTH [49].

SUA GUI displays the raster plot of multiple spike trains and the stimulus, if presented. Number of parameter selections for ISIH and PSTH such as Bin Size and pre and post stimulus duration for the PSTH display, are available in SUA GUI. NeuroQuest also provides a curve fitting tool for the ISIH that validates the quality of spike trains. ISTH of a typical neuron demonstrates a single negative exponential distribution with the empty first few bins of the histogram due to the refractory period, and the curve fitting tool verifies the quality of the spike train by fitting the distribution of the ISIH with exponential distribution [6],[5].

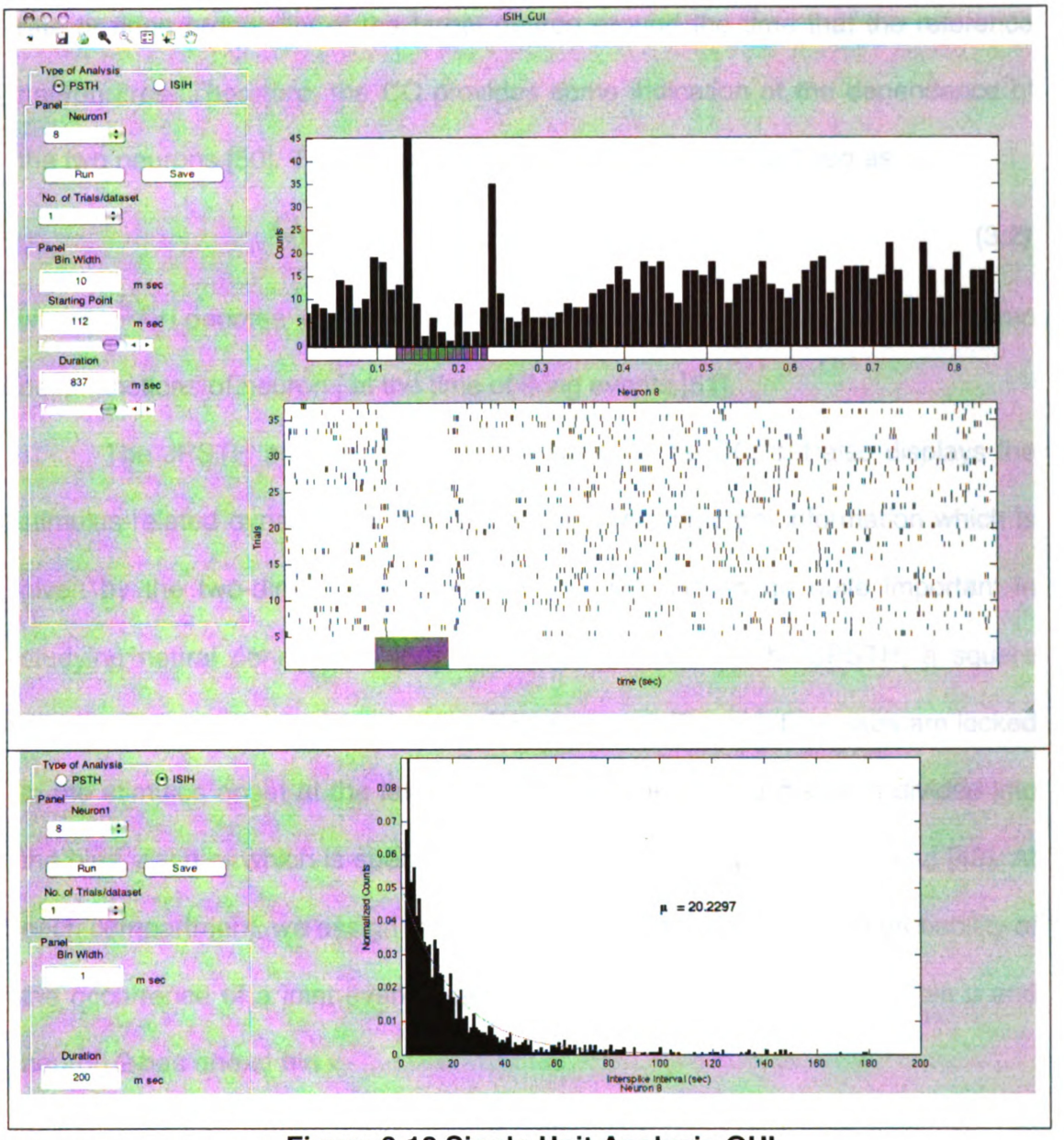

Figure 3-12 Single Unit Analysis GUI

3.3.5.2 Multi Unit Analysis tools.

The cross-correlogram (CC) is a function which indicates the firing rate of the target neuron versus the reference neuron. CC give some measure of the firing

rate or firing probability of the target neuron around the time that the reference neuron fires. Therefore, the CC provides some indication of the dependence of the two neurons [50]. The cross-correlation function can be defined as

$$Q_{i,j}(\tau) = E_t[(s_i(n)s_j(n+\tau)] \tag{3.2}$$

where $E_t[\bullet]$ denotes expected value over time n, and $s_j()$ is a sum of Dirac delta functions of neuron j at the time of firing events [51].

The JPSTH provides not only the ability of the CC, but also displays the stimulus-related dynamics of the relationship. The temporal information which is given by the two-dimensional nature of the JPSTH can be quite important in studying neural connectivity [50]. In the computation of the JPSTH, a square matrix with a size of the trial duration T is prepared. The two time axes are locked to the stimulus onset at the left-bottom corner. The square matrix is divided into the bins, each of which is specified by a pair of two integer indices (u, v) [49]. At each compartment, we assign the matrix element that quantifies the probability of the occurrence of a joint event, where neuron 1 has a spike event at bin u and neuron 2 has one at bin v,

$$\langle n_{12}(u,v)\rangle = \frac{1}{K}\sum_{k=1}^{K} n_{12}^{(k)}(u,v) \tag{3.3}$$

where

$$n_{12}^{(k)}(u,v) = n_1^{(k)}(u)n_2(k)(v) \tag{3.4}$$

Similar to SUA GUI, MUA GUI also provides the number of parameter selections for both JPSTH and CC such as Bin Size, Window Size for CC, and pre and post stimulus duration for the JPSTH display.

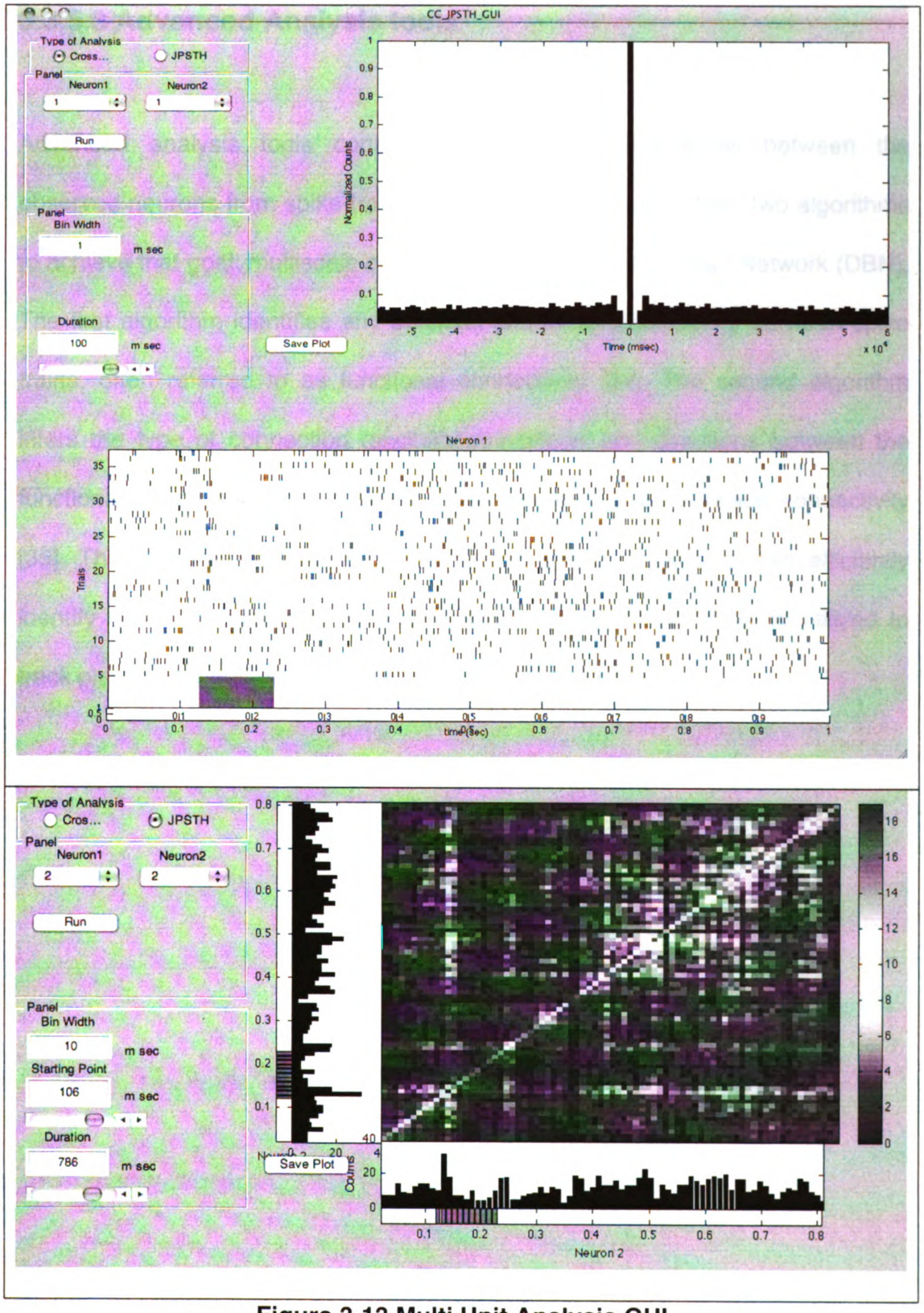

Figure 3-13 Multi Unit Analysis GUI

3.3.5.3 Advanced Analysis tools

Advanced analysis tools consist of identifying relationships between the observed neurons from spike train ensembles. NeuroQuest offers two algorithms to achieve that goal: multiscale clustering and Dynamic Bayesian Network (DBN). The first algorithm identifies any potential statistical dependency between spike trains, often referred to as functional connectivity [34]. The second algorithm infers the type of connection (excitatory/inhibitory) and directions between the functionally-interdependent neurons, often referred to as effective connectivity [35]. This is achieved through DBN. This two-stage framework can efficiently identify neural circuits in large neuronal populations. It can also be utilized to track plastic changes associated with learning and memory.

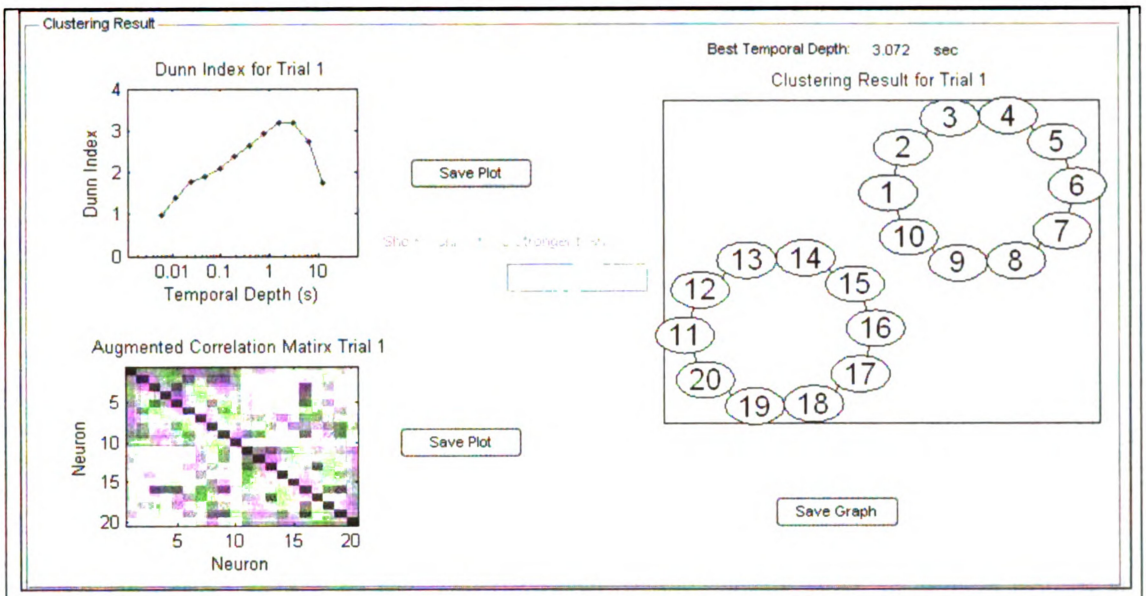

(a) Functional connectivity Estimation GUI

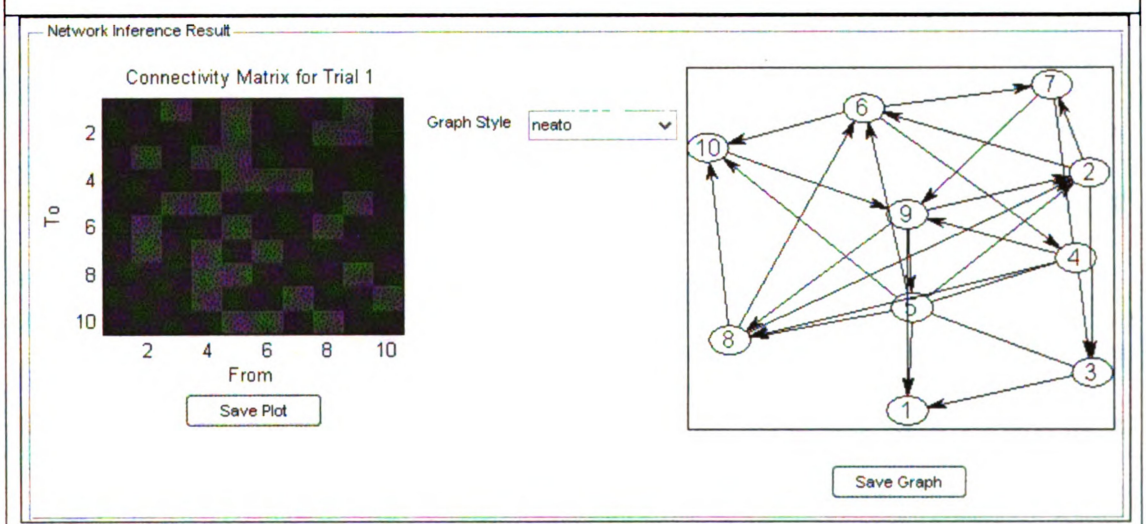

(b) Effectiveness Connectivity Estimation GUI

Figure 3-14 Advanced Spike Train Analysis GUI

CHAPTER 4

Spike Detection and Feature Extraction

4.1 Introduction

Spike detection refers to the identification of the arrival time of action potential waveforms produced by a neuron during active communication with other neurons in the nervous system. It is believed that spike arrival times carry all the information about information processing and not the actual waveform shape. Therefore extracting this temporal information is the first step to analyze neural recordings [7].

Extracellular recordings are corrupted by many noise components such as thermal and electrical noise, caused by signal amplifiers and other components of the data acquisition system, background neural activity, and the occasional similarity between the spike waveforms and the background noise [44]. Spikes are non-stationary over a long period of time due to many reasons such as electrode shifting, cell migrate, etc, and non-stationary background noise makes the presence of spikes unclear. The goal of spike detection is to obtain temporal information believed to be the most important parameter of neural activity from the noisy extracellular recordings [7].

Many spike detection algorithms were proposed to overcome these difficulties and they can be categorized as supervised or unsupervised, manual or automated methods [7],[19],[18],[44].

In this study, we focus only on automated and unsupervised detection methods. The simplest detection method is the amplitude threshold detection method which identifies any signal that crosses the threshold as a spike. Even though this method is simple, the detection performance is sensitive to noise. Energy-based spike detectors compare the local power of the signal with a threshold estimated from the power of noise [19]. This method is more robust to noise than the amplitude threshold method.

The wavelet method has been motivated as an alternative to threshold or energy based detection methods. Wavelet-based spike detection methods transform the extracellular recordings into multiple sparse representation spaces and compare them to a threshold. Wavelet-based spike detection methods were suggested due to the sparsity they introduce and therefore plays an important role in spike detection by increasing the signal-to-noise ratio (SNR) and localizing transients in extracellular recordings [18],[44].

However the sparsity in wavelet detection methods requires a rule for threshold selection because the distribution of the test statistic is not trivial to derive. This causes a complexity in automating the detection methods, and the threshold selection inevitably relies on an empirical approach.

Another problem of current wavelet detection methods is the relatively high

computational complexity due to the redundant detection routines in entire or selected wavelet subspaces. In wavelet domain, spikes are represented in relevant subspaces, and the general wavelet methods detect the spikes from each subspace separately and combine the detection results either by majority voting or logically OR them [44],[21]. Under this detection scheme, a single spike is detected multiple times creating a redundant detection.

In conventional spike sorting algorithm, detected spikes are extracted and properly aligned to obtain the feature set for spike sorting. These time consuming steps require to store entire recording or segments of detected spikes which is undesirable in large-scale neural data process.

In this chapter we propose a novel spike detection method using sparse representation in wavelet domain. Combining information scattered across multiple wavelet subspaces can reduce redundant detection. The proposed threshold selection method modifies the distribution of the observation to maximize separability between the noise and the signal distributions. We also propose the feature extraction method that captures the compact representation of the transient of the signal, called wavelet footprint. Under the proposed feature extraction scheme, a compact feature set is obtained at the same time detecting spikes that eliminates spike extraction and alignment steps as shown in figure 4-1.

The proposed wavelet detection method incorporated with the threshold selection was tested and the results were compared to several commonly used

spike detection methods. The proposed methods outperformed other methods in low SNR cases, and the wavelet footprint extraction method reduced the several steps in conventional spike sorting method: spike extraction, alignment and feature extraction, while keeping the desired separability of clusters for the spike sorting. Under the proposed wavelet footprint detection, significant amount of data reduction can be achieved for offline processing.

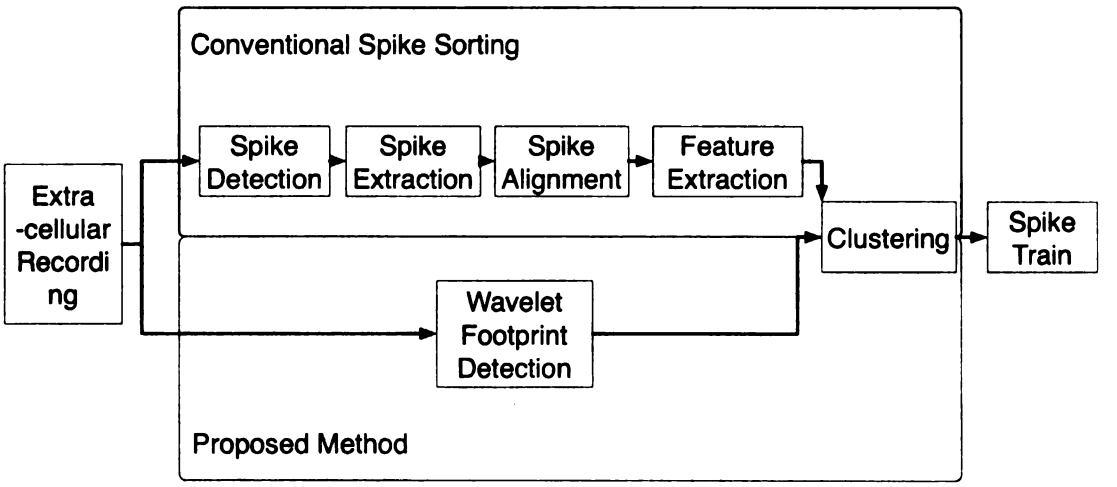

Figure 4-1. Block Diagram of the proposed wavelet footprint detection method.

4.2 Theory

4.2.1 Observation Model

We formulate spike detection as a binary hypothesis test problem, where

under the null hypothesis $\mathcal{H}_0$ the signal is not present, while under hypothesis $\mathcal{H}_1$ the signal is present

$$\mathcal{H}_0 : y[n] = z[n] \quad n = 0, 1, \ldots, N-1$$
$$\mathcal{H}_1 : y[n] = x[n] + z[n] \quad n = 0, 1, \ldots, N-1 \qquad (4.1)$$

where $y \in \Re^{1\times N}$ is the observation, $x \in \Re^{1\times N}$ is action potentials from single source, and $z \in \Re^{1\times N}$ is a white Gaussian noise with $z \sim \mathcal{N}(0, \sigma^2)$ where *N* is the number of samples in time domain [44].

Sparse representation of a transient signal has advantages in spike detection mainly because it maximizes the SNR by characterizing non-transient samples of the signal with large number of small coefficients, while discontinuities of the signal with small number of large coefficients. Second, the sparse representation tends to be highly localized in time domain, and this characteristic makes the detection robust to variations in spike durations. Transforms that yield the most compact representation of the signal are also desired to maximize the spike detection performance, and wavelet-based techniques demonstrate compact representation with precise frequency and time localizations [44].

4.2.2 Wavelet Transform and its Properties

Wavelet ψ, also called a mother wavelet, is a function of oscillation with finite energy and zero mean. A family of wavelet can be obtained by scaling and translating the mother wavelet [40]

$$\psi_{a,b}(t) = \frac{1}{\sqrt{a}}\psi\left(\frac{t-b}{a}\right) \quad a, b \in \mathbf{R} \tag{4.2}$$

where a > 0 is the scale and b is the translation.

The projection of a random signal y(t) onto the subspace of scale a has the form

$$y^{(a)}(t) = \int_{\mathbf{R}} y(t)\psi_{a,b}(t)dt \tag{4.3}$$

where $y^{(a)}(t)$ is the sparse representation of the signal y(t), a wavelet coefficient, at the ath wavelet subspace [40].

The wavelet transform has several attractive properties for signal and image processing [47]. Locality allows the wavelet atom localized simultaneously in time and frequency, and Compression transforms real-world signals to sparse representation. Persistence is a propagating tendency of wavelet coefficients across scales, and it is the key property supporting the proposed method [47]. Since a sparse representation of a spike propagates across multiple subspaces, there will be a redundancy across the relevant subspaces. Measuring the

correlation among the subspaces can capture the redundant representation of a single spike, and this can reduce the number of detection routines.

To maximize the correlation, wavelet coefficients must be invariant among different subspaces, and Stationary Wavelet Transform (SWT), designed to achieve the translation-invariance, satisfies our need for this study [40]. Figure 4-2 shows the sparse representation of spikes in wavelet domain and the properties of wavelet are clearly illustrated.

Now we derive the model in wavelet domain. By the linearity of SWT at scale j, observation y can be expressed as

$$y^{(j)} = yw^{(j)}$$
$$y^{(j)} = xw^{(j)} + zw^{(j)} = x^{(j)} + z^{(j)} \tag{4.4}$$

where $y^{(j)} \in \Re^{1\times N}$ is wavelet coefficients at jth subspace and $w^{(j)}$ is a corresponding wavelet base [44]. With L level wavelet domain transform, the two hypotheses in (4.1) have the following form:

$$\mathcal{H}_0 : \underline{y}[n] = \underline{z}[n] \; n = 0, 1, \cdots, N-1$$
$$\mathcal{H}_1 : \underline{y}[n] = \underline{x}[n] + \underline{z}[n] \;\; n = 0, 1, \cdots, N-1 \tag{4.5}$$

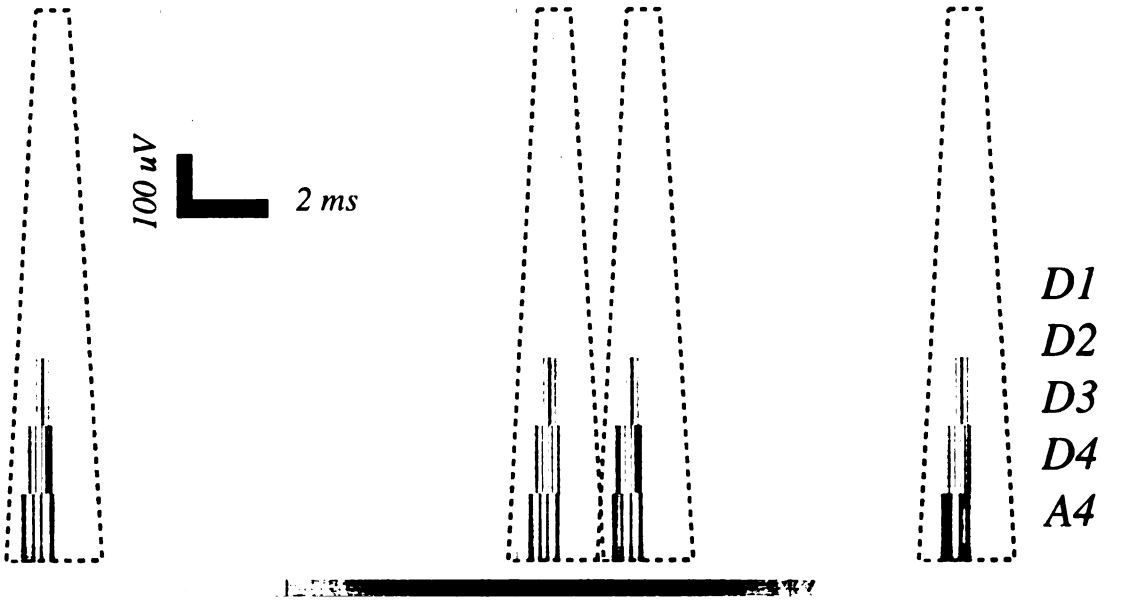

Figure 4-2. Sub-space representation of action potentials in wavelet domain The signal is transformed into 4 level wavelet domains using SWT and sym4 wavelet base. D and A denote detail and approximate nodes of SWT, respectively, and the number indicates level.

$$\begin{aligned} \underline{y}[n] &= [y^{(1)}[n], \ldots, y^{(L)}[n]] \\ \underline{x}[n] &= [x^{(1)}[n], \ldots, x^{(L)}[n]] \\ \underline{z}[n] &= [z^{(1)}[n], \ldots, z^{(L)}[n]] \end{aligned} \tag{4.6}$$

where y[n], x[n], and z[n] are a snapshot of wavelet coefficients of the observation, the spikes, and the noise, respectively, across multiple subspaces at time n.

Let $\mathcal{R}(\mathcal{H}_0|\underline{y})$ and $\mathcal{R}(\mathcal{H}_1|\underline{y})$ be the conditional risks associated with accepting and rejecting the hypothesis $\mathcal{H}_0$ given the evidence y respectively. These risks can be expressed as

$$\begin{aligned} \mathcal{R}(\mathcal{H}_1|\underline{y}) &= \lambda_{00}P(\mathcal{H}_0|\underline{y}) + \lambda_{01}P(\mathcal{H}_1|\underline{y}) \\ \mathcal{R}(\mathcal{H}_0|\underline{y}) &= \lambda_{10}P(\mathcal{H}_0|\underline{y}) + \lambda_{11}P(\mathcal{H}_1|\underline{y}) \end{aligned} \tag{4.7}$$

$\lambda_{(ij)} = \lambda(\mathcal{H}_i|\mathcal{H}_j)$ is the loss incurred for deciding $\mathcal{H}_j$ when the true state of nature is $\mathcal{H}_i$. Since correct decisions are not penalized, λ_{00} and λ_{11} are zero. This leads new expression of conditional risks described as $\mathcal{R}(\mathcal{H}_1|\underline{y}) = \lambda_{01}P(\mathcal{H}_1|\underline{y})$ and $\mathcal{R}(\mathcal{H}_0|\underline{y}) = \lambda_{10}P(\mathcal{H}_0|\underline{y})$. The fundamental rule is to decide $\mathcal{H}_1$, if $\mathcal{R}(\mathcal{H}_1|\underline{y}) < \mathcal{R}(\mathcal{H}_0|\underline{y})$ and vice versa. After invoking the Bayes rule $P(\mathcal{H}_i|\underline{y}) = P(\underline{y}|\mathcal{H}_i)/P(\underline{y})$, the decision rule becomes

$$\frac{P(\underline{y}|\mathcal{H}_1)}{P(\underline{y}|\mathcal{H}_0)} \underset{\mathcal{H}_0}{\overset{\mathcal{H}_1}{\gtrless}} \frac{\lambda_{01}}{\lambda_{10}} \frac{P(\mathcal{H}_1)}{P(\mathcal{H}_0)} \triangleq \eta \tag{4.8}$$

Note that η represents the acceptance threshold for $\mathcal{H}_1$. Under the unsupervised detection scheme, the covariance matrices of the signal and the noise are unknown and they can be estimated from the observation. Under the assumption that the noise is Gaussian we have $P(\underline{y}|\mathcal{H}_0) \sim \mathcal{N}(0, \Sigma)$ and $P(\underline{y}|\mathcal{H}_1) \sim \mathcal{N}(\pm\mu, \Sigma)$ where μ is the L-component mean vector of the signal $\underline{x}$ and Σ is the L-by-L covariance matrix of the observation. The generalized likelihood ratio test (GLRT) can be expressed as [45]

$$\underline{y}^T \Sigma^{-1} \underline{y} \gtrless_{\mathcal{H}_0}^{\mathcal{H}_1} 2 \log \eta \tag{4.9}$$

This is essentially a blind energy detector [44]. The sufficient statistic T for spike detection is

$$T = \underline{y}^T \Sigma^{-1} \underline{y} \tag{4.10}$$

4.2.3 Optimal Threshold Selection for a χ2 Distributed Signal

The threshold η in (4.9) is estimated considering the costs of false detection and a priori probability of $\mathcal{H}_0$ and $\mathcal{H}_1$ [27]. Since information about the true action potentials and the noise is unknown in unsupervised detection, η is estimated as mean and variance of the observation [52]. Median Absolute Deviation (MAD) is used to estimate the noise variance, but it is only valid with a Gaussian noise assumption [52]. Since the square of a random variable with a normal distribution is χ2 distribution, the sufficient statistic T in (4.10) is χ2 distributed. χ2 distribution is a special case of a gamma distribution expressed as

$$f_v(x) = \frac{1}{\Gamma(\frac{v}{2}) 2^{\frac{v}{2}}} x^{\frac{v}{2}-1} exp(\frac{v}{2}) \tag{4.11}$$

with a scale parameter β = 2, where $\Gamma(\alpha) = (\alpha - 1)!$, a shape parameter α = v/2, and v being the degree of freedom of the random variable x.

An optimal threshold must be selected to maximize the positive detection rate and to minimize the false detection rate [27]. Figure 4-3.a and 4-3.b illustrate the probability density function (PDF) and the cumulative distribution function (CDF) of χ2 distribution for different v. Since T is a combination of the χ2 distributed signal and noise with the parameter v close to 1, discriminating one from another is not easy. Figure 4-4.a illustrates the χ2 distribution of the sufficient statistic *T*. Red bars represent histogram of noise and black bars correspond to the signal. There is no clear separation between the two distributions.

A modification of the histogram of *T* helps to estimate the threshold. Histogram equalization (HE) is a method of contrast adjustment in image processing using the histogram of the image [53]. This method increases the global contrast of the image presented by close contrast value by linearizing the cumulative distribution function (CDF) [53]. Linearization of the CDF to lead an increase in the parameter v. If the HE shifts v from 1 to 3 or larger values, the distributions of the noise and the signal are separable as shown in figure 4.3.a. The general HE at bin index k is expressed as

$$h(k) = \frac{cdf(k) - cdf_{min}}{cdf_{max} - cdf_{min}} \times (L - 1) \tag{4.12}$$

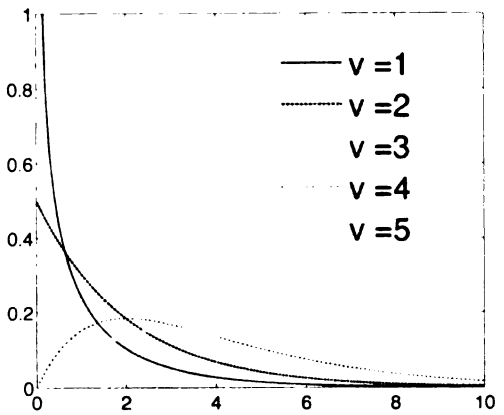

a) PDF of χ2 distribution

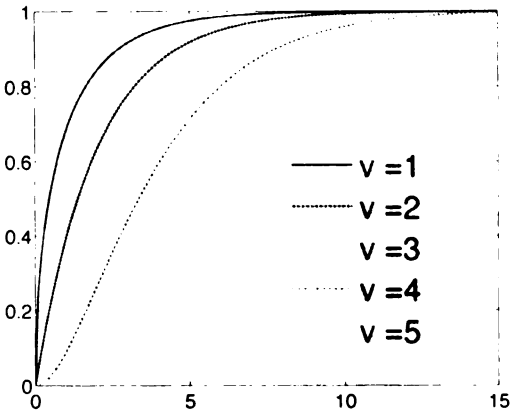

a) CDF of χ2 distribution

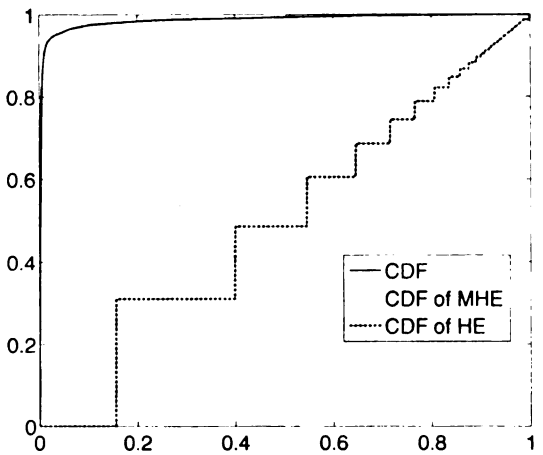

c) CDP of the three histograms

Figure 4-3. PDF and CDF of X2 distribution with different parameter v and ›the equalized CDPs using the general histogram equalization (HE) and the modified histogram equalization (MHE)

where cdf_{min} being the minimum of CDF, and cdf_{max} being the maximum of CDF, L being a total number of bins. However the regular HE method creates a significant quantization distortion in the case of χ2 distribution with v=1 as shown in figure 4-3.c. The modified HE (MHE) for χ2 distribution is expressed as

$$h'(k) = \begin{cases} (cdf(k) - cdf(k-1)) \times k & k > 1 \\ cdf(k) \times k & k = 1 \end{cases} \quad (4.13)$$

The MHE yields much smoother linearization of the CDF of χ2 distributed signal with v=1. Once the histogram is equalized using the MHE, the histogram is transformed into the modified histogram (MH) with v greater than 1 where the separation between the noise and signal is more favorable.

Figure. 4-4.b shows the modified histogram of T that has a clear separation between the noise and the signal distributions. The estimated threshold is located at a local minimum between the two peaks. This is similar to the gray-level histogram threshold selection in image processing [54].

4.2.4 Wavelet Footprint

The discontinuous structures of a signal often carry critical information, thus efficient characterization of the discontinuity of the signal is a central task in signal processing [47]. In general, larger wavelet coefficients tend to be around the edge of a signal and these wavelet coefficients collect most of the energy of the original signal. A wavelet footprint is defined as scale space vectors obtained by gathering all the wavelet coefficients around the discontinuities of the signal that model discontinuities in piecewise polynomial signal exactly [47].

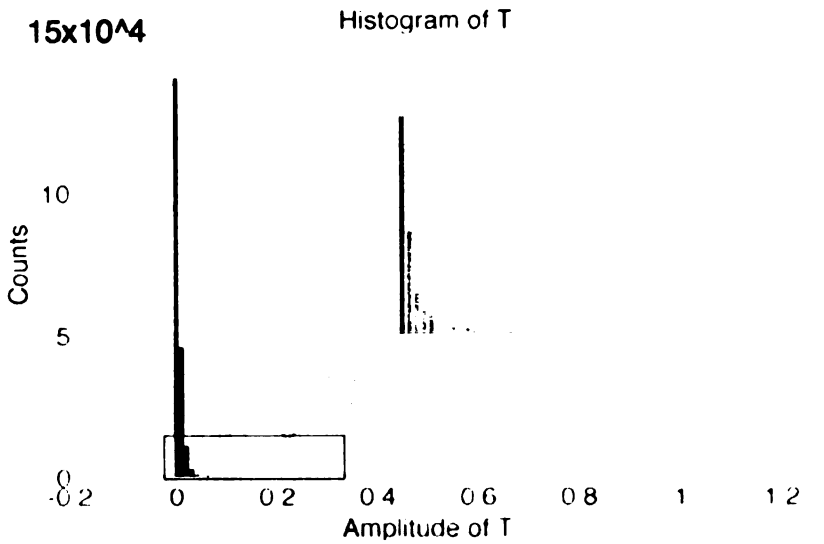

(a) Histogram of sufficient statistic T

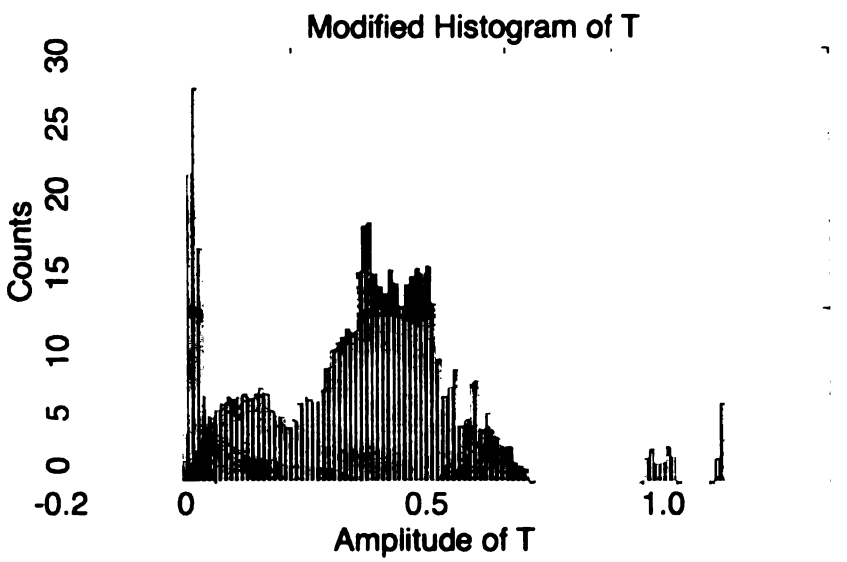

(b) The Modified Histogram of sufficient statistic T

Figure 4-4. Histogram and modified histogram of sufficient statistic T (a) The histogram illustrates the sparsity of T. Bright colored bars represent noise while dark ones represent signals. (b) The modified histogram of T is shown.

Given a piecewise constant signal y with only one discontinuity at position k, wavelet footprint $f_k^{(0)}$ is the scale-space vector obtained by gathering together the largest wavelet coefficient from each node in the cone of influence of k.

This footprint $f_k^{(0)}$ can be written as

$$f_k^{(0)} = [max(y^{(1)}[k - \frac{D_1}{2} : k + \frac{D_1}{2}], \cdots, max(y^{(L)}[k - \frac{D_L}{2} : k + \frac{D_L}{2}]] \quad (4.14)$$

where D_i is duration of the cone of influence of i^{th} subspace at k. The cone of influence (COI) is the region of the wavelet spectrum in which edge effects become important and details of COI are found in [40].

We can expand the feature extraction method from the single channel case to multi-channel data set when high correlations between neighboring channels is present by concatenating a footprint from single channel together with ones from other channels into one event vector, a long feature vector can consolidate all the information in three domains: time, scale and space. Figure 4-5 demonstrates how the method can be applied to multi- channel data.

4.3 Results

To evaluate the performance of the presented spike detection and the threshold selection methods, simulated datasets with different SNRs were used. For

comparison, the datasets were obtained from OSort, a spike detection and sorting package [11]. Stimulated datasets were generated by using a database of

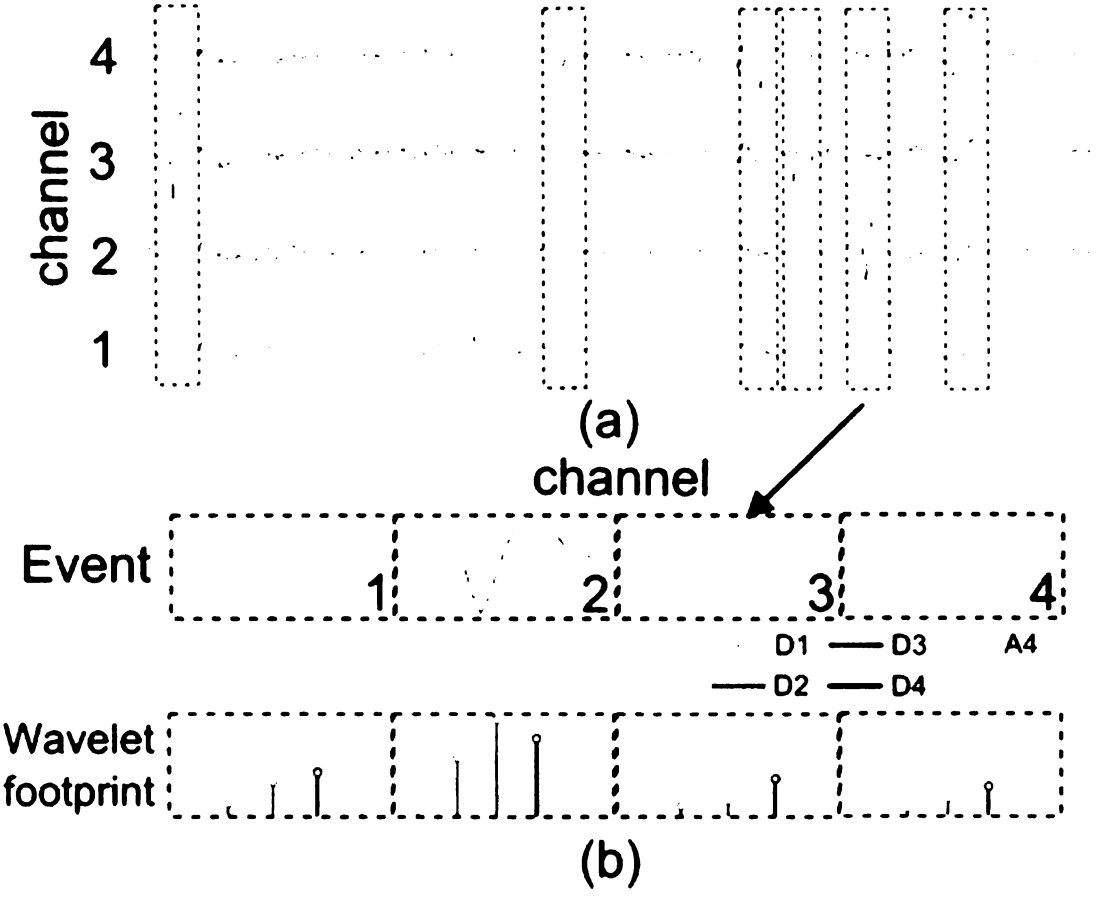

Figure 4-5 Wavelet footprint extraction method for the correlated multi-channel signal. (a) Multi-channel data. A spike event, a snapshot of neural action potential across the multi channels, is extracted and forms a vector of event. (b) Wavelet footprint extraction from an event vector. Different colors indicate specific nodes of SWT.

150 mean waveforms taken from well-separated neurons recorded in previous experiments. The random background noise is generated by selecting randomly scaled spike waveforms from the database and added to the noise traces. Identifiable spikes are added by simulating a number of neurons (3 in dataset 1

and2, and 5 in dataset 3), with a renewal Poisson process with a refractory period 3ms and a fixed firing rate between 1 to 10 HZ [11]. The proposed detection algorithm was fully implemented in NeuroQuest, a software package for neural data analysis, and all the results were obtained using NeuroQuest [55].

First, receiver operating characteristic (ROC) curves were plotted to examine the detection accuracy of each method. The SNR was calculated as the root-mean square (RMS) of the spike divided by the standard deviation of the observation [11]. Three commonly used spike detection methods, single amplitude detection (SAD) with a single threshold, absolute amplitude detection (AAD) with both positive and negative thresholds, energy-based detection (EBD), and the proposed wavelet detection (WD) were used for the comparison. For the WD, the observation signal was transformed into wavelet domain using 5-level SWT with a symlet 4 wavelet base. The sufficient statistic T was estimated from D2 to D4 where D denotes a detail node of wavelet transform, because typical action potentials have frequency range between 1 KHz to 5 KHz. From Figure 4-6, SAD performed poorly, while WD performed better than the other methods in the lowest SNR cases.

We compared two different threshold selection methods, the proposed modified histogram equalization (MHE), and the MAD. For the comparison, we used 3 and 5 times of the MAD, because other wavelet and energy based detection methods typically estimate the detection threshold with 3 or 5 times of

the MAD [11]. The results shown in figure 4-7 illustrate the robustness of MHE method in low SNR cases.

We compared the spike detection performance with EBD. EBD was selected for the comparison because of its robust detection performance from the ROC test and the $\chi 2$ distributed EBD samples that the MHE method can be applied to.

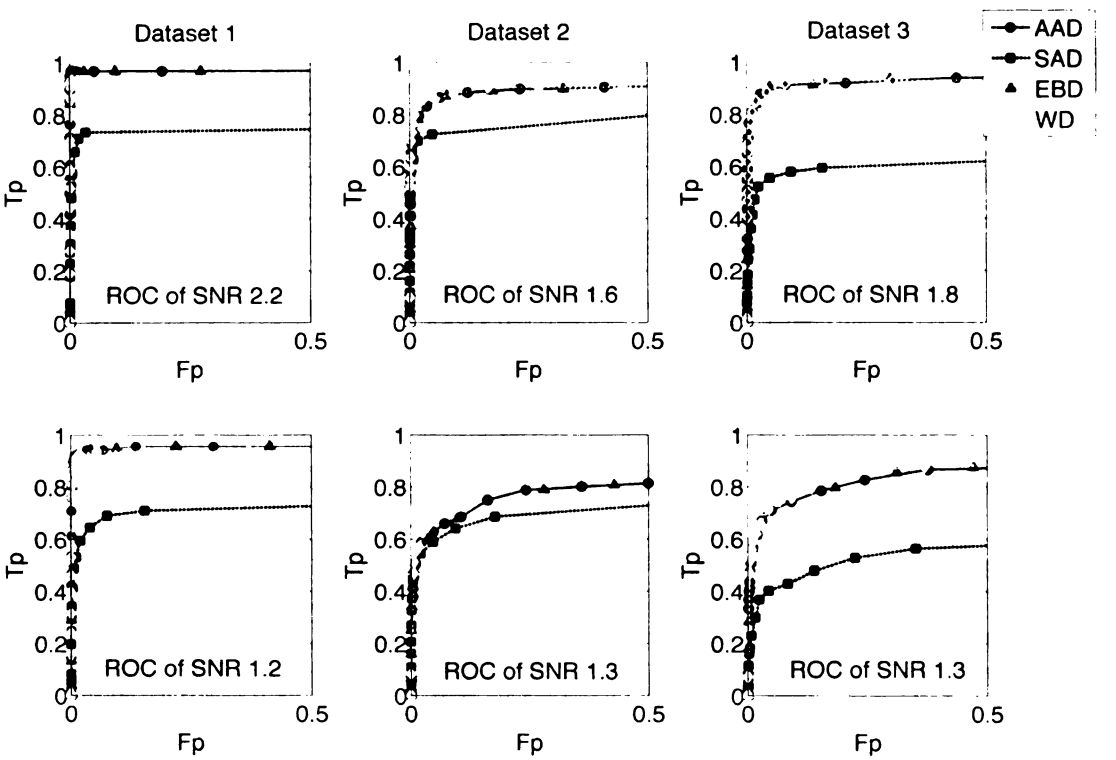

Figure 4-6. ROC for different datasets with different SNR AAD: absolute amplitude detection, SAD: single amplitude detection, EBD: energy-based detection, WD: the proposed wavelet detection. Tp and Fp denote True Positive and False Positive respectively. Each column represents ROC of different dataset and each raw represents different SNR.

TABLE 4-1. SPIKE DETECTION RESULTS OF EBD AND WD

Dataset3 (2986)	SNR:5.4	SNR:2.7	SNR:1.8	SNR:1.3
EBD + 5 x MAD	TP:100% FP: 0%	TP:98.6% FP: 6%	TP:91.3% FP: 12%	TP:76.1% FP: 33%
EBD + MH	TP:98.6% FP: 0%	TP:93.5% FP: 2%	TP:64.1% FP: 1%	TP:54.4% FP: 2%
WD + 5 x MAD	TP:96.4% FP: 1%	TP:95.3% FP: 5%	TP:93.5% FP: 48%	TP:80% FP: 54%
WD + MH	TP:96.4% FP: 1%	TP:96.7% FP: 1%	TP:75.4% FP: 1%	TP:58.3% FP: 3%

Dataset 3 was used for the comparison. There are 2986 spikes in the dataset 3. TP and FP represent true positive and false positive of detection, respectively. FP rate is calculated by the number of false detection divided by the maximum false detection with a detection threshold value at 0.

Four different combinations of two detection methods and two threshold selection methods were tested. From the result shown in Table 4-1, we conclude that WD is robust to the noise and MH yields low false detection rate for high positive detection rate. In the highest SNR case, however, the performance of WD was lower than EBD. The reason was that a small number of overlapped spikes were represented as a single spike in the wavelet domain.

We examined the spike sorting result using the wavelet footprint feature set. Once spikes were detected, the wavelet footprint was obtained by extracting a local maximum of each subspace within the cone of influence of the detected spike. Since the typical duration of single spike is 1-2 ms, the range of the cone of influence is $K \pm D/2$, where K is being a position of the detected local maximum and D being total samples equivalent to 2ms. D in this study was 50 with 25kHz of the sampling rate.

(a) Raw dataset3 with SNR 5.4 in time domain

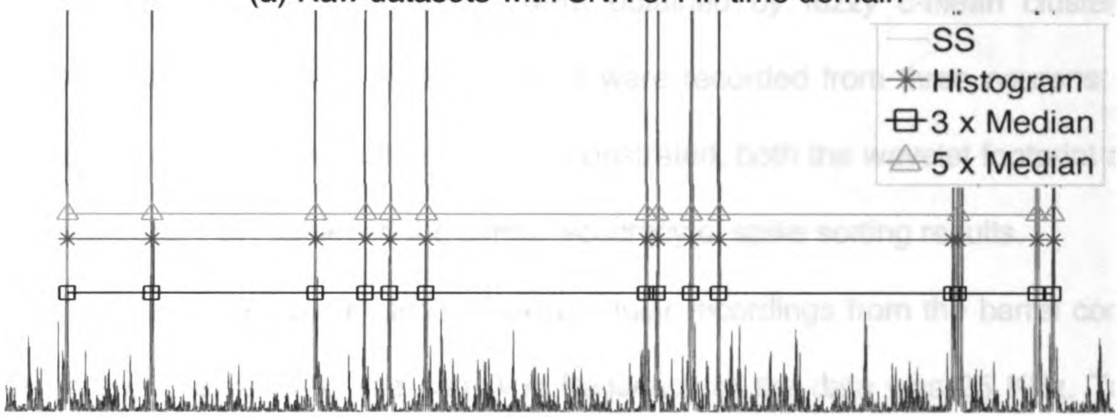

(b) Corresponding Sufficient Statistic of subspace redundancy and different threshold selection methods

(c) Raw dataset3 with SNR 1.8 in time domain

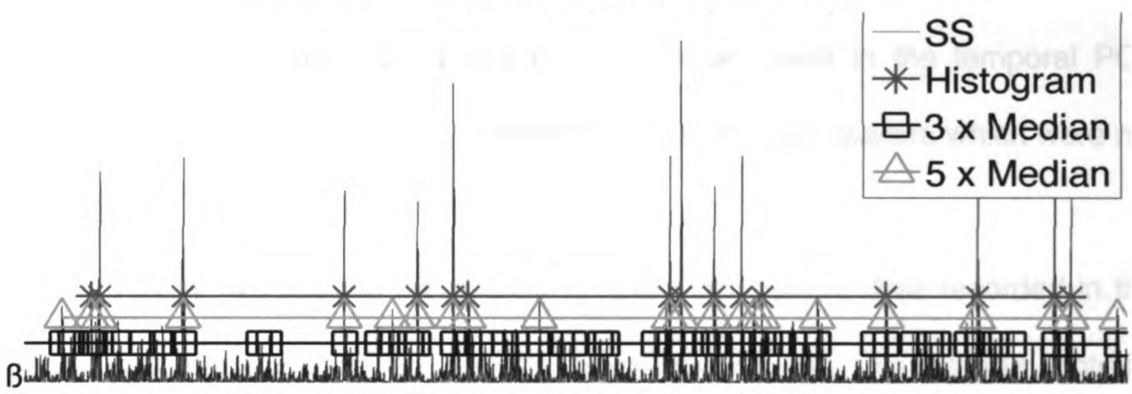

(d) Corresponding Sufficient Statistic in subspace redundancy and different threshold selection methods

Figure 4-7. Sufficient statistic T of the segment of dataset 3 and the different threshold selections Markers indicated the detection points with the corresponding thresholds.

The spike sorting result of two feature sets - the wavelet footprint and the entire spike waveform - were compared. First, we tested the method with simulation data set that consists of two independent recordings. For display purposes, we selected only the largest two principle components of each feature set. All the spike sorting results were obtained by fuzzy c-mean clustering method. Both Channel 1 and channel 2 were recorded from three neurons. As the confusion matrices in figure 4-8 demonstrated, both the wavelet footprint and the temporal PCA achieved the similar accuracy of spike sorting results.

We applied the method to extracellular recordings from the barrel cortex of an anesthetized rat. The sampling frequency of the data was 25 KHz. Total 1849 spikes were detected, and the spike sorting results with the temporal PCA and the wavelet footprints were compared. The results of spike sorting are shown in figure 4-9. Three clear clusters were identified in temporal PCA, while four clusters were identified in the wavelet footprint. The identified clusters in the wavelet footprint were more scattered than those found in the temporal PCA which is not desirable. However it helped to separate two clusters which were not separable in the temporal PCA.

Finally, we applied the method to the multi-channel data recorded in the dorsal cochlear nucleus of an anesthetized Guinea pig. The wavelet footprint feature set was obtained as described in section 4.2.4, and the temporal PCA feature set was extracted from the concatenated spike waveform extracted from the each channel of the array.

TABLE 4-2. CONFUSION MATRICES OF THE SPIKE SORTING RESULTS

Channel 1	Neuron 1 (181)	Neuron 2 (159)	Neuron 3 (25)	**Channel 2**	Neuron 1 (173)	Neuron 2 (190)	Neuron 3 (32)
Classified Neuron1	97.5% (95.1%)	1(0)	0	Classified Neuron1	100% (100%)	2 (7)	0
Classified Neuron2	2 (4)	98.3% (100%)	0	Classified Neuron2	0	98% (93%)	0
Classified Neuron3	0	0	100% (100%)	Classified Neuron3	0	0	100% (100%)

( ) indicates the sorting result using the wavelet footprint feature set. Confusion matrices show the similar spike sorting results of both feature sets.

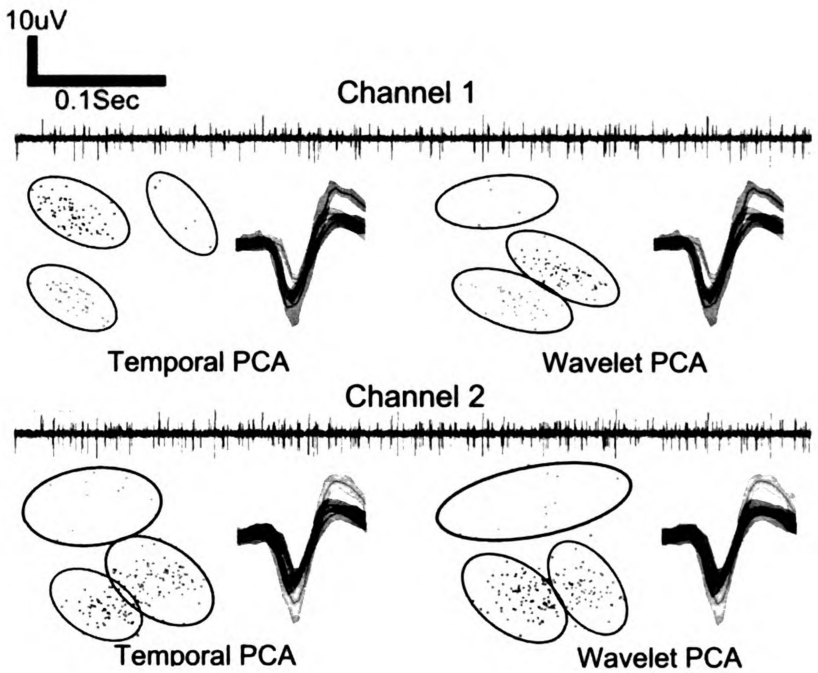

Figure 4-8 Clusters of temporal PCA and the wavelet footprint Raw signals, feature spaces in temporal PCA and wavelet footprint, and templates of sorted spikes. Channel 1 and 2 are recorded from three different neurons. Color indicates links between spike templates and clusters.

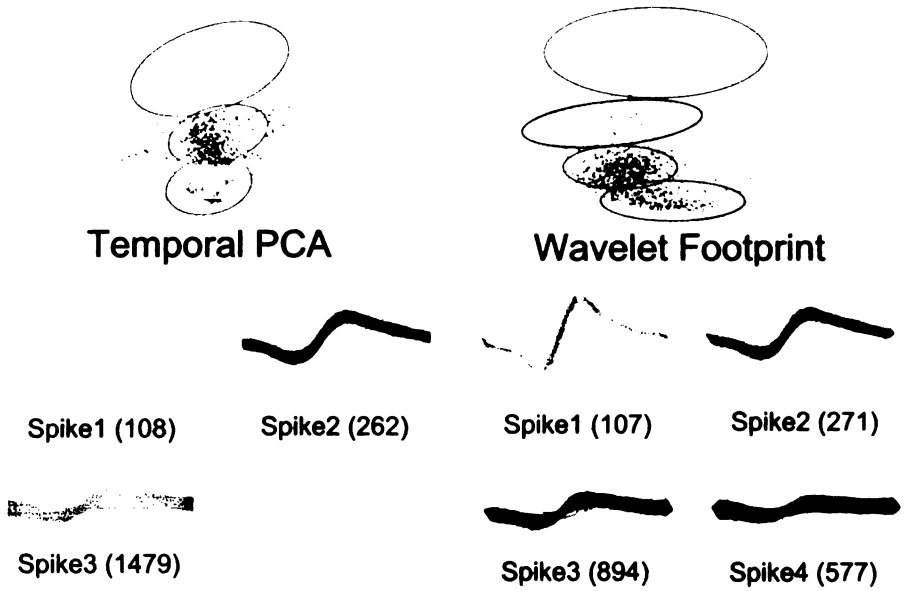

Figure 4-9 Spike sorting results of spontaneous recordings from an anesthetized rat. 3 units are identified in Temporal PCA, whereas 4 units are found in wavelet footprint domain. Spike 3 in temporal PCA can be further separated into two units, spike 3 and spike 4 in the wavelet footprint domain.

For comparison, we fixed the number of clusters 6 and used the fuzzy-c mean clustering method. As figure 4-10 illustrated, the two different feature spaces displayed similar distribution. This implies that wavelet footprint feature set shares the similar variation with the actual spike waveform, because PCA is a projection of the data onto the eigenvector that has the direction of the largest variation in the data [27]. This is an indication of the effective feature extraction performance of wavelet footprint that can achieve a significant amount of data reduction, 90% of compression rate per spike sampled at 25KHz.

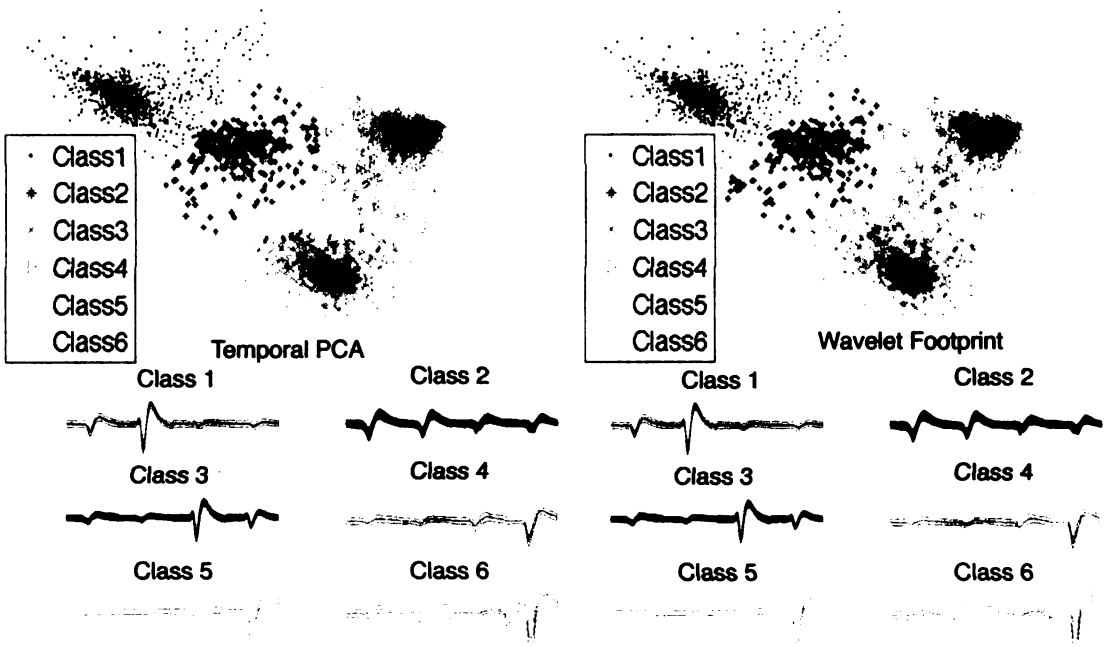

Figure 4-10 Spike sorting result of the multi-channel dataset The color-coded clusters match with the corresponding spike waveforms. The width of the shaded area in the spike waveform indicates the variance. Clusters and the sorted spike waveforms in two different feature spaces, temporal PCA and wavelet footprint, have similar distribution. This result implies that the wavelet footprint is the effective sparse representation of the data.

4.4 Conclusion

Sparse representation of the extracellular recordings is key to achieve reliable spike detection in low SNR, and the wavelet transform exhibits advantages in characterizing these signals. We presented two contributions: 1) a novel spike detection method, capturing the correlations across multiple subspaces, and 2) the threshold selection, modifying the distribution of the observation to maximize

the separability between the noise and the signal. The proposed detection method demonstrated improved detection performance in low SNRs.

We also have shown the simultaneous feature extraction method using wavelet footprints, a sparse feature set that captures the information across scales. Many different data sets including actual recorded data from anesthetized animals were tested to verify the effectiveness of the method. The entire spike waveform and the wavelet footprint feature set demonstrated very similar distributions in PCA domain among many different data sets. Since the size of wavelet footprint feature set is one tenth of the entire spike waveform, a massive reduction in data transmission and storage can be achieved. The proposed method also eliminates multiple processing steps in the conventional spike sorting algorithm which is crucial step to implement the algorithm into a realtme online sorting.

APPENDIX

Appendix A

NeuroQuest Input Data Structure

NeuroQuest works with a MAT file that contains a specific data structure.

The data file must have

- data: A cell array that each cell contains 1 sec raw data.
- BinWidth: Inverse of the sampling rate. 1/(sampling rate)
- chanInfo: channel labels. It is a raw vector. Ex) Four channel data with channel index 1,3,5,7. chanInfo = [1 3 5 7];
- plotOption: a structure array that contains seven components (raw, denoise, detection, stimulus, LFP, spiketrain, and Trials). plotOption is a set of flags that indicates types of data the file contains. If a data file has only raw data, plotOption.raw is 1 and other values are 0.
- fileDescription: a cell array that contains a short description of the data.

All the labels are case-sensitive and missing components will cause an error.

BIBLIOGRAPHY

BIBLIOGRAPHY

[1] M. Scanziani and M. Hausser, "Electrophysiology in the age of light," *Nature*, vol. 461, Oct. 2009, pp. 930-939.

[2] G. Buzsaki, *Rhythms of the Brain*, Oxford University Press, USA, 2006.

[3] "MEASUREMENTS OF VISUAL EVOKED POTENTIALS IN PARKINSON'S DISEASE," Dec. 1978.

[4] A.M. Kuncel and W.M. Grill, "Selection of stimulus parameters for deep brain stimulation," *Clinical Neurophysiology*, vol. 115, Nov. 2004, pp. 2431-2441.

[5] R.E. Kass, V. Ventura, and E.N. Brown, "Statistical Issues in the Analysis of Neuronal Data," *J Neurophysiol*, vol. 94, Jul. 2005, pp. 8-25.

[6] E.N. Brown, R.E. Kass, and P.P. Mitra, "Multiple neural spike train data analysis: state-of-the-art and future challenges," *Nature Neuroscience*, vol. 7, May. 2004, pp. 456-461.

[7] M.S. Lewicki, "A review of methods for spike sorting: the detection and classification of neural action potentials," *Network: Computation in Neural Systems*, vol. 9, 1998, p. 53.

[8] K.D. Harris, *KlustaKwik. Automatic Cluster Analysis, version 1.0*, 2002.

[9] C. Fraley and A.E. Raftery, "MCLUST: Software for model-based cluster analysis," *Journal of Classification*, vol. 16, 1999, pp. 297-306.

[10] R.Q. Quiroga, Z. Nadasdy, and Y. Ben-Shaul, "Unsupervised spike detection and sorting with wavelets and superparamagnetic clustering," *Neural computation*, vol. 16, 2004, pp. 1661-1687.

[11] U. Rutishauser, E.M. Schuman, and A.N. Mamelak, "Online detection and sorting of extracellularly recorded action potentials in human medial temporal lobe recordings, in vivo," *Journal of neuroscience methods*, vol. 154, 2006, pp. 204-224.

[12] K.G. Oweiss, *Statistical Signal Processing for Neuroscience and Neurotechnology*, Elsevier, in Press.

[13] E.C. Leuthardt, G. Schalk, J.R. Wolpaw, J.G. Ojemann, and D.W. Moran, "A brain–computer interface using electrocorticographic signals in humans," *Journal of Neural Engineering*, vol. 1, 2004, pp. 63-71.

[14] W.H. Pilcher and W.G. Rusyniak, "Complications of epilepsy surgery," *Neurosurgery Clinics of North America*, vol. 4, Apr. 1993, pp. 311-325.

[15] K.J. Miller, M. denNijs, P. Shenoy, J.W. Miller, R.P. Rao, and J.G. Ojemann, "Real-time functional brain mapping using electrocorticography," *NeuroImage*, vol. 37, Aug. 2007, pp. 504-507.

[16] A.D. Legatt, J. Arezzo, and H.G. Vaughan, "Averaged multiple unit activity as an estimate of phasic changes in local neuronal activity: effects of volume-conducted potentials," *Journal of Neuroscience Methods*, vol. 2, Apr. 1980, pp. 203-217.

[17] K.G. Oweiss, "A systems approach for data compression and latency reduction in cortically controlled brain machine interfaces," *IEEE Transactions on Bio-Medical Engineering*, vol. 53, Jul. 2006, pp. 1364-1377.

[18] X. Yang and S.A. Shamma, "A totally automated system for the detection and classification ofneural spikes," *IEEE Transactions on Biomedical Engineering*, vol. 35, 1988, pp. 806-816.

[19] Kyung Hwan Kim and Sung June Kim, "Neural spike sorting under nearly 0-dB signal-to-noise ratio using nonlinear energy operator and artificial neural-network classifier," *IEEE Transactions on Biomedical Engineering*, vol. 47, Oct. 2000, pp. 1406-1411.

[20] K.G. Oweiss and D.J. Anderson, "Tracking signal subspace invariance for blind separation and classification of nonorthogonal sources in correlated noise," *EURASIP Journal on Advances in Signal Processing*, vol. 2007, 2007.

[21] Z. Nenadic and J.W. Burdick, "Spike detection using the continuous wavelet transform," *IEEE Transactions on Biomedical Engineering*, vol. 52, 2005, pp. 74-87.

[22] M.S. Fee, P.P. Mitra, and D. Kleinfeld, "Variability of extracellular spike waveforms of cortical neurons," *J Neurophysiol*, vol. 76, Dec. 1996, pp. 3823-3833.

[23] M.S. Fee, P.P. Mitra, and D. Kleinfeld, "Automatic sorting of multiple unit neuronal signals in the presence of anisotropic and non-Gaussian variability," *Journal of Neuroscience Methods*, vol. 69, 1996, pp. 175-188.

[24] T. Hermle, C. Schwarz, and M. Bogdan, "Employing ICA and SOM for spike sorting of multielectrode recordings from CNS," *Journal of Physiology-Paris*, vol. 98, 2004, pp. 349-356.

[25] J.C. Bezdek and R. Ehrlich, "FCM: The fuzzy c-means clustering algorithm," *Computers & Geosciences*, vol. 10, 1984, pp. 191-203.

[26] S. Shoham, M.R. Fellows, and R.A. Normann, "Robust, automatic spike sorting using mixtures of multivariate t-distributions," *Journal of neuroscience methods*, vol. 127, 2003, pp. 111-122.

[27] R.O. Duda, P.E. Hart, and D.G. Stork, *Pattern Classification*, Wiley-Interscience, 2000.

[28] S. Takahashi, Y. Anzai, and Y. Sakurai, "A new approach to spike sorting for multi-neuronal activities recorded with a tetrode--how ICA can be practical," *Neuroscience research*, vol. 46, 2003, pp. 265-272.

[29] K.G. Oweiss and D.J. Anderson, "MASSIT-Multiresolution Analysis of Signal Subspace InvarianceTechnique: a novel algorithm for blind source separation," *Signals, Systems and Computers, 2001. Conference Record of the Thirty-Fifth Asilomar Conference on*, 2001.

[30] J.D. Victor and K.P. Purpura, "Metric-space analysis of spike trains: theory, algorithms and application," *Network: Computation in Neural Systems*, vol. 8, 1997, p. 127.

[31] G. Palm, A. Aertsen, and G.L. Gerstein, "On the significance of correlations among neuronal spike trains," *Biological Cybernetics*, vol. 59, 1988, pp. 1-11.

[32] G.E.P. Box, G.M. Jenkins, and G.C. Reinsel, *Time series analysis: forecasting and control.*

[33] A.M. Aertsen, G.L. Gerstein, M.K. Habib, and G. Palm, "Dynamics of neuronal firing correlation: modulation of "effective connectivity"," *J Neurophysiol*, vol. 61, May. 1989, pp. 900-917.

[34] S. Eldawlatly, R. Jin, and K.G. Oweiss, "Identifying functional connectivity in large-scale neural ensemble recordings: A multiscale data mining approach," *Neural computation*, vol. 21, 2009, pp. 450-477.

[35] S. Eldawlatly, Y. Zhou, R. Jin, and K.G. Oweiss, "On the use of dynamic bayesian networks in reconstructing functional neuronal networks from spike train ensembles," *Neural computation*, vol. 22, 2010, pp. 158-189.

[36] R. Meier, U. Egert, A. Aertsen, and M.P. Nawrot, "FIND--A unified framework for neural data analysis," *Neural Networks*, vol. 21, 2008, pp. 1085-1093.

[37] H. Bokil, P. Andrews, H. Maniar, B. Pesaran, J. Kulkarni, C. Loader, and P. Mitra, "Chronux: a platform for analyzing neural signals," *BMC Neuroscience*, vol. 10, 2009, p. S3.

[38] A.S. Sedra and P.O. Brackett, *Filter theory and design: active and passive*, Matrix Pub, 1978.

[39] P.G. Musial, S.N. Baker, G.L. Gerstein, E.A. King, and J.G. Keating, "Signal-to-noise ratio improvement in multiple electrode recording," *Journal of Neuroscience Methods*, vol. 115, Mar. 2002, pp. 29-43.

[40] S.G. Mallat, *A wavelet tour of signal processing*, Academic Pr, 1999.

[41] K.G. Oweiss, "Multiresolution analysis of multichannel neural recordings in the context of signal detection, estimation, classification and noise suppression," Rice University, 2002.

[42] S.G. Chang, B. Yu, and M. Vetterli, "Adaptive wavelet thresholding for image denoising and compression," *IEEE Transactions on Image Processing*, vol. 9, 2000, pp. 1532-1546.

[43] D.L. Donoho, "De-noising by soft-thresholding," *IEEE transactions on information theory*, vol. 41, 1995, pp. 613-627.

[44] K.G. Oweiss, "Multiresolution analysis of multichannel neural recordings in the context of signal detection, estimation, classification and noise suppression," Rice University, 2002.

[45] Y. Suhail, "Methods for neural signal processing and analysis," MICHIGAN STATE UNIVERSITY, 2005.

[46] A. Pavlov, V.A. Makarov, I. Makarova, and F. Panetsos, "Separation of Extracellular Spikes: When Wavelet Based Methods Outperform the Principle Component Analysis," *Mechanisms, Symbols, and Models Underlying Cognition*, 2005, pp. 123-132.

[47] P.L. Dragotti and M. Vetterli, "Wavelet footprints: Theory, algorithms, and applications," *IEEE Transactions on Signal Processing*, vol. 51, 2003, pp. 1306-1323.

[48] M.A.T. Figueiredo and A.K. Jain, "Unsupervised Learning of Finite Mixture Models," *IEEE TRANSACTIONS ON PATTERN ANALYSIS AND MACHINE INTELLIGENCE*, vol. 24, 2000, pp. 381--396.

[49] H. Ito and S. Tsuji, "Model dependence in quantification of spike interdependence by joint peri-stimulus time histogram," *Neural computation*, vol. 12, 2000, pp. 195-217.

[50] P. Dayan, L.F. Abbott, and L. Abbott, *Theoretical neuroscience: Computational and mathematical modeling of neural systems*, MIT Press, 2001.

[51] C.K. Knox, "Cross-correlation functions for a neuronal model," *Biophysical Journal*, vol. 14, 1974, pp. 567-582.

[52] D.L. Donoho and J. JOHNSTONE, "Ideal spatial adaptation by wavelet shrinkage," *Biometrika*, vol. 81, 1994, p. 425.

[53] S.M. Pizer, E.P. Amburn, J.D. Austin, R. Cromartie, A. Geselowitz, T. Greer, B. ter Haar Romeny, J.B. Zimmerman, and K. Zuiderveld, "Adaptive histogram equalization and its variations," *Computer vision, graphics, and image processing*, vol. 39, 1987, pp. 355-368.

[54] N. Otsu, "A threshold selection method from gray-level histograms," *Automatica*, vol. 11, 1975, pp. 285-296.

[55] K.Y. Kwon, S. Eldawlatly, and K.G. Oweiss, "NeuroQuest: A Comprehensive Tool for Large Scale Neural Data Processing and Analysis," *4th Int IEEE EMBS*, Turkey: 2009, pp. 622-625.